Study of the decay pattern of $f_0(1370)$ as a $\kappa\bar{\kappa}$ molecular state

Yin Cheng[1,*] and Bing-Song Zou[2,†]

[1]*Institute of Theoretical Physics, Chinese Academy of Sciences, Beijing 100190, China*
[2]*Department of Physics and Center for High Energy Physics, Tsinghua University, Beijing 100084, China*

(Received 5 March 2026; accepted 15 July 2026; published 9 September 2026)

Under the hypothesis that the $f_0(1370)$ is a $\kappa\bar{\kappa}$ molecular state, we calculate the partial widths of its various decay channels, including the two-body decays $K\bar{K}$, $\pi\pi$, and $\eta\eta$ and the four-body decays $\rho\rho/\sigma\sigma \to 4\pi$ and $K\bar{K}\pi\pi$. Treating the coupling $g_{f_0(1370)\kappa\bar{\kappa}}$ as a free parameter, we find that a value of 25–40 GeV brings the total width of $f_0(1370)$ in line with the measured value 200–500 MeV. At the center-of-mass energy $\sqrt{s} = 1.37$ GeV, the channels that mainly contribute to the total width are $K\bar{K}$, $\pi\pi$, and 4π ranked as $\Gamma(K\bar{K}) > \Gamma(4\pi) > \Gamma(\pi\pi)$ with $g_{f_0(1370)\kappa\bar{\kappa}} = 35$ GeV. Around 1.37 GeV, the decay widths of the two-body channels $K\bar{K}$, $\pi\pi$, and $\eta\eta$ remain stable with variation in $\sqrt{s}$, whereas the decay widths of the four-body channels 4π and $K\bar{K}\pi\pi$ increase continuously with $\sqrt{s}$. Most current data are model dependent and conflicting, particularly regarding the conclusion of 4π dominance and the ratio of $K\bar{K}$ to $\pi\pi$ decay widths. The current data cannot rule out the $\kappa\bar{\kappa}$ assignment for $f_0(1370)$. Further reliable theoretical and experimental analyses of $f_0(1370)$ are required to reveal its nature.

DOI: 10.1103/wz77-w51n

I. INTRODUCTION

Quantum chromodynamics (QCD) was established as the theory of strong interaction almost 50 years ago. However, its low-energy regime is still not well understood due to the breakdown of perturbation theory, particularly the scalar spectrum below 2 GeV. The strange mass pattern of the lightest scalars $f_0(500)$, also called σ, $a_0(980)$, $f_0(980)$ contradicts the quark model description, which raises some exotic assignment for them, such as molecular state and tetraquark state [1–7]. It seems that the scalars above 1 GeV should be assigned to the lowest 0^{++} $q\bar{q}$ nonet, which are expected to be heavier than the lowest pseudoscalars and vectors due to its $^3P_0$ configuration. However, the set of particles possibly filled into this nonet seems to be supernumerary and their mass ordering is also anomalous as shown in the review of particle physics (RPP) [8]. The properties of the $f_0(1500) - f_0(1370)$ are incompatible with them being the singlet-octet system in $q\bar{q}$ nonet. If $f_0(1370)$ is considered as dominantly $n\bar{n}$ state then the $s\bar{s}$ state is expected to be 200–300 MeV heavier and decay strongly into $K\bar{K}$, while the partial widths of $f_0(1500)$ decaying into $\pi\pi$ and 4π are dominant. Its decay ratio to $K\bar{K}$ is only $8.5 \pm 1.0\%$ as reported in the RPP [8].

In light of this phenomenology, earlier Amsler and Close [9,10] suggested that the scalars $f_0(1370)$, $f_0(1500)$, and $f_0(1710)$ can originate from a mixing scheme of the scalar glueball with the scalar $q\bar{q}$ state. Subsequently, numerous works have been devoted to the different glueball mixing schemes [11–14].

On the other hand, some studies on the meson-meson interactions suggest that the $f_0(1370)$ may be dynamically generated in the isoscalar $\rho\rho$ S-wave interaction [15–17]. However, when the $\pi\pi$ and $K\bar{K}$ coupled channels are included, Ref. [18] claims that the $\rho\rho$ resonance aligns more closely with the $f_0(1500)$, based on its pole position and partial decay widths. Assigning the $f_0(1500)$ and $f_0(1710)$ as $\rho\rho$ and $K^*\bar{K}^*$ molecular states, respectively, Ref. [19] has investigated their plausible isospin partners $a_0(1450)$ and $a_0(1710)$. In the present work, we use the term "molecule" loosely to refer to a state whose formation is governed by a dominant meson-meson component, rather than requiring the strict weak-binding condition of a bound state lying just below the corresponding threshold.

It is worth mentioning that the signal of $f_0(1370)$ in experiments is subtle and controversial. In 1966, a measurement of the 4π spectrum in the $\bar{p}n \to 2\pi^+3\pi^-$ process [20] found a deviation from the phase space distribution, which is explained by a scalar $\rho\rho$ resonance with mass $m = 1.41$ GeV and width $\Gamma = 90$ MeV. RPP

*Contact author: chengyin@itp.ac.cn
†Contact author: zoubs@mail.tsinghua.edu.cn

Published by the American Physical Society under the terms of the Creative Commons Attribution 4.0 International license. Further distribution of this work must maintain attribution to the author(s) and the published article's title, journal citation, and DOI. Funded by SCOAP³.

lists this data as an observation of $f_0(1370)$ [8]. The width in this analysis is too narrow compared to those in other analyses of $f_0(1370)$, which is about 300 MeV, but it is consistent with the average width of $f_0(1500)$. A reanalysis of $\bar{p}n \to 2\pi^+3\pi^-$ by Gaspero [21] shows that this reaction is dominated by a 4π resonance with mass $m = 1386$ MeV, width $\Gamma = 310$ MeV, and quantum number $I^G J^{PC} = 0^+0^{++}$, which decays to both $\rho^0\rho^0(29\%)$ and $\sigma\sigma\,(71\%)$. A compatible scalar was observed in $p\bar{p} \to \pi^+\pi^-3\pi^0$ by Crystal Barrel Collaboration [22], which decays through both $\rho^+\rho^-$ and $\sigma\sigma$ intermediate states with different relative strengths for these two decay modes. The discrepancy is natural because the comparison is made between the ratios of $\rho^0\rho^0/\sigma\sigma$ and $\rho^+\rho^-/\sigma\sigma$. Later measurements of $\bar{p}d \to \pi^-4\pi^0 p$ require two scalar states, $f_0(1370)$ and $f_0(1500)$ [23], with mass and width parameters consistent with prior results. While analyses of Crystal Barrel data of 4π [23,24] indicate strong coupling of the $f_0(1370)$ to the 4π final state, studies of its two-body decays have produced highly contradictory results. This is further complicated by the $f_0(1500)$, a $\rho\rho$ molecule candidate that is expected to dominate the 4π spectrum. Therefore, the $f_0(1370)$ signal in the 4π spectrum is still ambiguous.

The Crystal Barrel data in Refs. [25–27] manifest a peak in the $\pi\pi$ and $\eta\eta$ S wave at about 1400 MeV, as well as a further peak at about 1560 MeV. Its width varies between 200 and 700 MeV, depending on theoretical models. A combined fit [28] to the Crystal Barrel data on $p\bar{p} \to 3\pi^0$, $\eta\eta\pi^0$, and $\eta\pi^0\pi^0$, which is fully consistent with several other sets of data: CERN-Munich data on $\pi^-\pi^+ \to \pi^-\pi^+$, GAMS data on $\pi^- p \to \pi^0\pi^0 n$, and data from ANL and BNL on $\pi^-\pi^+ \to K\bar{K}$, claimed that the $f_0(1370)$ is definitely required by the data on $3\pi^0$ and $\eta\pi^0\pi^0$, as well as $\pi\pi \to K\bar{K}$.

Klempt and Zaitsev [29,30] question the existence of $f_0(1370)$. They argue that in the $\eta\eta$ spectra in $p\bar{p}$ annihilation at higher primary energy [31–33], $f_0(1500)$ is always observed clearly but they argue that in the $\eta\eta$ spectra from $\bar{p}p$ annihilation at higher primary energies [31–33], $f_0(1500)$ is always clearly observed, but no such "direct" evidence for $f_0(1370)$ is found. However, $f_0(1370)$ might have weaker decay rate to the $\eta\eta$ channel compared to $f_0(1500)$, and as stated in [33] the resonances near the boundaries of the Dalitz plot suffer from the effect of the anticuts. Five primary sets of data requiring $f_0(1370)$ are refitted with suitable Breit-Wigner amplitudes by Bugg to further confirm its existence [34].

The partial waves analyses from $\pi^- p \to K\bar{K}n$ and $\pi^+ n \to K^-K^+p$, i.e., the $\pi\pi \to K\bar{K}$ scattering, at ANL [35–37] and BNL [38] favored the solution requiring an f_0 enhancement around 1300 MeV. Moreover, a model-independent dispersive analysis on $\pi\pi$ scattering data claims the confirmation of the existence of $f_0(1370)$ [39].

For the pp central production, an early measurement of $\pi^+\pi^-$ system by WA102 Collaboration [40] claimed that it was not possible to describe the data above 1 GeV without the addition of both the $f_0(1370)$ and $f_0(1500)$ resonances. Similar results were obtained from a coupled-channel analysis [41] of centrally produced K^+K^- [42] and $\pi^+\pi^-$ [40] final states. A relatively recent data from STAR Collaboration [43] on pp central production of $\pi^+\pi^-$ and K^+K^- also claim the possible contribution from $f_0(1370)$ in addition to the $f_0(1500)$. Based on the WA102 measurements in pp central production, the ratio of $f_0(1370) \to K\bar{K}$ to $f_0(1370) \to \pi\pi$ is determined to be 0.46 ± 0.19 [41,44].

For the production in J/ψ radiative decays, Ref. [45] found convincing evidence of the existence of $f_0(1370)$ in J/ψ and $\psi(2S)$ radiative decay, although only in the $K\bar{K}$ decay channel. Due to limited statistics, partial-wave analysis was not performed in [45]. Consequently, the $f_0(1370)$ signal in the $\pi\pi$ channel is obscured by the strong excitation of nearby $f_2(1270)$. However, partial-wave analyses of higher-statistics $J/\psi \to \gamma\pi^0\pi^0$ [46] and $J/\psi \to \gamma K_S K_S$ [47] data both reveal a clear 0^{++} structure around 1.4 GeV. A coupled-channel analysis [48] including these two data sets obtains the branching ratios $\mathrm{Br}(J/\psi \to \gamma f_0(1370) \to \gamma\pi\pi) = (3.8 \pm 1) \times 10^{-4}$ and $\mathrm{Br}(J/\psi \to \gamma f_0(1370) \to \gamma K\bar{K}) = (1.3 \pm 0.4) \times 10^{-4}$. The authors in Ref. [48] claim that the interference between neighboring states plays a decisive role and the change in the sign of the coupling constant in $\pi\pi$ and $K\bar{K}$ decays for $f_0(1500)$ with respect to the $f_0(1370)$ "background" has first been noticed in Ref. [49].

For the production in J/ψ hadronic decays, BESIII has measured the $\omega K\bar{K}$ [50], $\omega\pi^+\pi^-$ [51], $\phi K\bar{K}$, and $\phi\pi\pi$ [52] spectra. The leading-order mechanism of J/ψ hadronic decay to $V(PP)$ suggests that the quark flavors within the recoiled meson V must appear in the resonance of the two pseudoscalars. No signals of $f_0(1370)$ or $f_0(1500)$ are observed in the $\omega K\bar{K}$ and $\omega\pi^+\pi^-$ spectra. However, the same as decaying to $\pi\pi$, a clear signal of $f_0(1370)$ is observed in the case of recoiling against ϕ. A chiral unitary coupled channel study of the meson-meson S wave interaction in Ref. [53] provides a successful description of the $f_0(1370)$ together with the other scalar-isoscalar resonances below 2 GeV and assigns $f_0(1370)$ as a pure SU(3) octet state $(u\bar{u} + d\bar{d} - 2s\bar{s})/\sqrt{6}$, not mixed with the glueball. This assignment would imply an $f_0(1370)$ signal in J/ψ hadronic decays recoiling against ω, which is not observed experimentally. Note that the study in Ref. [53] does not include the data from J/ψ hadronic decay, which could provide a further test of their octet assignment for $f_0(1370)$.

In the $\phi K\bar{K}$ data, there is a shoulder on its upper side that may be fitted by the interference between $f_0(1500)$ and $f_0(1710)$, but no conspicuous enhancement of $f_0(1370)$ is observed. Therefore, a ratio of $\mathrm{Br}(J/\psi \to \phi f_0(1370) \to \phi K\bar{K})/\mathrm{Br}(J/\psi \to \phi f_0(1370) \to \phi\pi\pi) = 0.08 \pm 0.08$ is presented, which is much lower than those reported by

the Review of Particle Physics. As discussed in Ref. [52], this discrepancy arises from the conspicuous signal in the $\pi\pi$ spectrum and the absence of any corresponding peak in the K^+K^- spectrum.

While numerous studies have advocated for the necessity of the $f_0(1370)$, most analyses to date rely on fits using sums of Breit-Wigner functions. This approach often produces reaction-dependent results, a problem particularly acute for the $f_0(1370)$ given its large width and proximity to the $f_0(1500)$ resonance.

Motivated by the phenomenology that the signals of $f_0(980)$, $f_0(1370)$, and $f_0(1790)$ appear successively in the $\pi\pi$ spectrum in J/ψ hadronic decay recoiling against ϕ, where the $s\bar{s}$ pair contributes to the (PP) resonance, we argue that the $f_0(1370)$ might be a $\kappa\bar{\kappa}$ molecular state, inspired by the $f_0(980)$ and $f_0(1790)$ being the plausible $K\bar{K}$ and $K^*\bar{K}^*$ molecules, respectively. In this work, we aim to investigate the decay pattern for the primary decay channels of $f_0(1370)$, including $\pi\pi$, $K\bar{K}$, $\eta\eta$, 4π, and $K\bar{K}\pi\pi$, within the framework where the $f_0(1370)$ is treated as a $\kappa\bar{\kappa}$ molecular state. Regardless of whether the components are broad or narrow, they are nearly free particles inside the molecular state in the weak-binding limit. Decay through the almost free components implies that the width of the bound state is expected to be of the same order of magnitude as the width of its components. This argument is illustrated by the case of the T_{cc}^+ discovered by LHCb [54], whose width is almost saturated by the decay via its constituents $D^*D \to DD\pi$ and is analyzed to be about 48 keV. The width of its constituent D^* is (83.4 ± 1.8) keV [8], of the same order as the T_{cc}^+ width, exemplifying the expected relation between the width of a hadronic molecule and the widths of its components. Hence, aligning with this argument the broad state $f_0(1370)$ is reasonably suspected to be a molecular state composed of $\kappa\bar{\kappa}$. In Sec. II, we present the decay mechanism and the detailed formalism for the calculation. In Sec. III, we will present the numerical results as well as the discussions. A brief summary will be given in Sec. IV.

II. FORMALISM

In this section, we present the detailed formalism for calculating the partial decay widths of the $f_0(1370)$ as a $\kappa\bar{\kappa}$ molecular state. Using the isospin conventions shown in Appendix A, we have

$$|\kappa^+\kappa^-\rangle\left|\frac{1}{2},\frac{1}{2}\right\rangle\left|\frac{1}{2},-\frac{1}{2}\right\rangle = \frac{1}{\sqrt{2}}|1,0\rangle + \frac{1}{\sqrt{2}}|0,0\rangle, \tag{1}$$

$$|\kappa^0\bar{\kappa}^0\rangle - \left|\frac{1}{2},-\frac{1}{2}\right\rangle\left|\frac{1}{2},\frac{1}{2}\right\rangle = -\left(\frac{1}{\sqrt{2}}|1,0\rangle - \frac{1}{\sqrt{2}}|0,0\rangle\right). \tag{2}$$

According to these isospin projections, the wave function of $f_0(1370)$ has the form of

$$f_0(1370) = \frac{1}{\sqrt{2}}|\kappa^+\kappa^-\rangle + \frac{1}{\sqrt{2}}|\kappa^0\bar{\kappa}^0\rangle. \tag{3}$$

Given that the κ is a broad resonance often modeled as a $K\pi$ molecule, considering two such broad states to form a molecular state is counterintuitive. However, this system can be essentially regarded as a $(K\pi)(\bar{K}\pi)$ four-body interacting system. To avoid the complexity of four-body dynamics, we argue that describing the system as a $\kappa\bar{\kappa}$ molecule is a reasonable and practical approximation. Within this framework, we evaluate whether the predicted decay pattern of the $f_0(1370)$ remains consistent with available experimental data. We emphasize that the predictions in this paper are inevitably subject to some model dependence.

Given the complexity of determining the coupling between $f_0(1370)$ and its broad κ components, we treat $g_{F\kappa\bar{\kappa}}$ [F denotes $f_0(1370)$ for brevity] as a free parameter in our model. The value of this coupling is taken as a parameter that is fitted to the measured total width of $f_0(1370)$. Specifically, based on the wave function the coupling $g_{F\kappa^+\kappa^-} = g_{F\kappa^0\bar{\kappa}^0} = (1/\sqrt{2})g_{F\kappa\bar{\kappa}}$. We set the coupling $g_{F\kappa\bar{\kappa}}$ as a real number in this work, since its phase does not matter for the issues we study here.

In the hadronic molecule picture, the schematic diagrams of $f_0(1370)$ decay to different channels, including $\pi\pi$, $K\bar{K}$, $\eta\eta$, 4π, and $K\bar{K}\pi\pi$, are shown in Fig. 1. Note that the vertices with quantum numbers SSP, SPV are forbidden and with quantum numbers SSS, SSV, SPP, SVV are allowed based on the parity conservation laws. For the allowed vertices, the adopted effective Lagrangians have the forms as

$$\mathcal{L}_{SSS} = g_{SSS}\langle SSS\rangle, \tag{4}$$

$$\mathcal{L}_{SPP} = g_{SPP}\langle SPP\rangle, \tag{5}$$

$$\mathcal{L}_{SVV} = g_{SVV}\langle V^\mu V_\mu S\rangle, \tag{6}$$

$$\mathcal{L}_{SSV} = ig_{SSV}\langle V^\mu[S,\partial_\mu S]\rangle, \tag{7}$$

where the symbol $\langle\ldots\rangle$ indicates the trace in the SU(3) flavor space. The overall couplings g_{SSS}, g_{SPP}, g_{SVV} have dimension of [mass] and g_{SSV} is a dimensionless constant. The detailed forms of the flavor SU(3) multiplets can be found in [55].

We use simple Breit-Wigner propagators for the K^* and ρ, which are relatively narrow states. However, for the scalar mesons deep into the complex plane the Breit-Wigner parametrization is not accurate. Hence, as shown in Fig. 1, the κ and σ appearing in the decay mechanism as intermediate states are represented as simple poles that are parametrized as

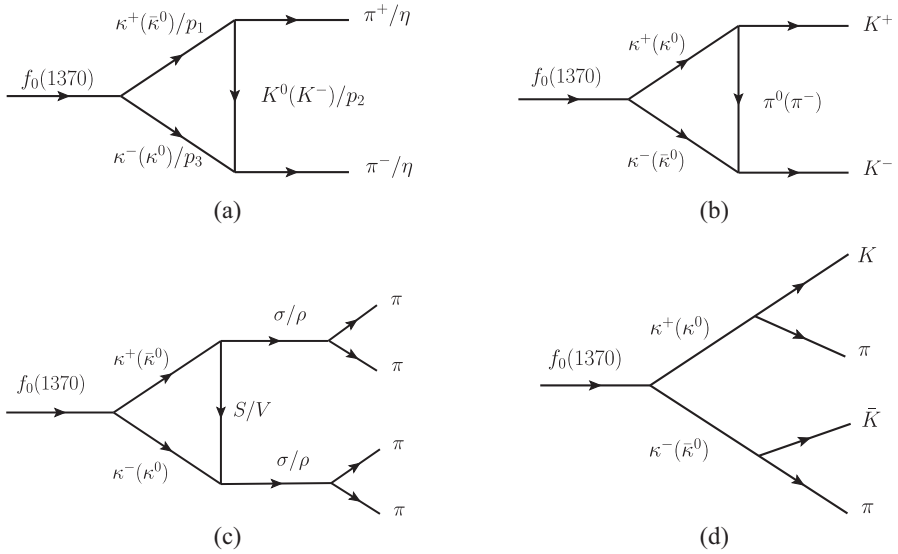


FIG. 1. Mechanism for $f_0(1370)$ decay as a $\kappa\bar{\kappa}$ molecular state. (a) $\pi^+\pi^-/\eta\eta$ final states. (b) K^+K^- final states. (c) 4π final states. S/V denotes that the t-channel exchange meson is either a scalar κ or a vector K^*. (d) $K\bar{K}\pi\pi$ final states.

$$G_\kappa(s) = \frac{1}{s - s_\kappa}, \qquad G_\sigma(s) = \frac{1}{s - s_\sigma}, \tag{8}$$

respectively, where s_κ and s_σ are, respectively, the squares of the pole positions: $\sqrt{s_\kappa} = m_\kappa - i\Gamma_\kappa/2$ with $m_\kappa = 0.7$ GeV, $\Gamma_\kappa = 0.6$ GeV, and $\sqrt{s_\sigma} = m_\sigma - i\Gamma_\sigma/2$ with $m_\sigma = 0.47$ GeV, $\Gamma_\sigma = 0.55$ GeV, the average values listed in the RPP [8].

It is important to note that several distinct mechanisms contribute to the same final states, particularly in the 4π channel. Consequently, the relative phases of the couplings must be explicitly taken into account to determine the interference pattern. Expanding the Lagrangian in Eq. (5) and focusing on the $\sigma\pi\pi$ vertex, we can obtain,

$$\mathcal{L}_{\sigma\pi\pi} = \frac{g_{SPP}}{\sqrt{2}} \cdot \sigma\pi^0\pi^0 + \sqrt{2} g_{SPP} \cdot \sigma\pi^+\pi^-. \tag{9}$$

Note that due to the identical feature, there are two ways to contract the two π^0 fields and the two final π^0 states for the first term. Based on this effective Lagrangian, the effective couplings are defined as follows: $g_{\sigma\pi^0\pi^0} = g_{SPP}/\sqrt{2}$ and $g_{\sigma\pi^+\pi^-} = \sqrt{2} g_{SPP}$. The effective couplings $g_{\kappa K\pi}$ and $g_{\sigma\pi\pi}$ we define here can be related to the residues at the resonance poles of κ in $K\pi$ scattering and σ in $\pi\pi$ scattering, respectively. We adopt the residue $\tilde{g}_{\sigma\pi\pi} = 3.61 e^{-1.30i}$ GeV for the σ pole from Refs. [56,57]. By transforming this coupling for $\pi\pi$ with fixed isospin $I = 0$ to the coupling associated with specific particles based on Eq. (B10), we have $g_{\sigma\pi^+\pi^-} = \tilde{g}_{\sigma\pi\pi}(-\sqrt{2}/\sqrt{3}) = -0.79 + 2.84i$ GeV and $g_{\sigma\pi^0\pi^0} = g_{\sigma\pi^+\pi^-}/2 = -0.39 + 1.42i$ GeV. Reference [56] also provides the coupling $\tilde{g}_{\rho\pi\pi} = 6.01 e^{-0.09i}$.

We adopt the residues $\tilde{g}_{\kappa^0 K\pi} = 3.81 e^{-1.49i}$ GeV and $\tilde{g}_{K^{*0} K\pi} = 5.69 e^{-0.076i}$ from Ref. [58]. Similarly, they can be transferred to the couplings associated with specific particles based on Eq. (B2): $g_{\kappa^0 K^+\pi^-} = \tilde{g}_{\kappa^0 K\pi}(\sqrt{2}/\sqrt{3}) = 0.25$–$3.10i$ and $g_{K^{*0} K^+\pi^-} = \tilde{g}_{K^{*0} K^+\pi^-}(\sqrt{2}/\sqrt{3}) = 4.63 - 0.35i$. Because the pole positions of ρ and K^* are relatively close to the real axis, their corresponding residues have small argument and are almost real numbers. The strength of coupling $|g_{K^{*0} K^+\pi^-}| = 4.64$ is very close to the strength of $g_{\phi K^+K^-}$ extracted from the decay of $\phi \to K\bar{K}$, e.g., $|g_{\phi K^+K^-}| = 4.47$ determined in Ref. [59]. Such a phenomenon is a confirmation of the flavor symmetry result that $g_{K^{*0} K^+\pi^-} = g_{\phi K^+K^-} = g_{VPP}$.

Now we turn to the discussion of the remaining relevant couplings. The magnitude of $g_{\sigma\pi^+\pi^-}$ adopted here is 2.95. Similarly, from the expanded Lagrangian we adopt that $g_{\sigma K\bar{K}} = g_{\sigma\pi^+\pi^-}/2$ under the SU(3) symmetry, leading to the ratio of $g_{\sigma K\bar{K}}/g_{\sigma\pi^+\pi^-}$ is 0.5. These couplings are also extracted in Ref. [60] by fitting the $\pi\pi \to \pi\pi/K\bar{K}$ scattering data with different models of K- and S matrices. They found the average value of $|g_{\sigma\pi^+\pi^-}| = 2.47 \pm 0.45$ GeV and about 0.6 ± 0.2 for the ratio of $g_{\sigma K\bar{K}}/g_{\sigma\pi^+\pi^-}$, both quantities are consistent with the our adopted values.

The $\sigma\kappa\kappa$ coupling can be approximately related to the $\sigma K\bar{K}$ and $\sigma\pi\pi$ couplings when the component π or K of the κ is considered as a spectator. Analogous estimations can be applied to the coupling $g_{\sigma\kappa\bar{K}^*}$ which can be related to the couplings $g_{K^{*0} K^+\pi^-}$, and the coupling $\rho\kappa\bar{\kappa}$, which can be related to the couplings $\rho\pi\pi$ and $\rho K\bar{K}$. The $\rho K^*\bar{\kappa}$ coupling can be related to another VVS type coupling $\sigma\rho\rho$ under flavor symmetry with coupling $g_{\sigma\rho^+\rho^-}$ determined by assuming $g_{\sigma\pi^+\pi^-} = g_{\sigma\rho^+\rho^-}$. For convenience, we collect the explicit formulas for estimating these couplings in Appendix B and list their specific values in Table I.

Based on these effective Lagrangians, the amplitude of the diagram in Fig. 1(a) decaying to $\pi^+\pi^-$ via the neutral

TABLE I. Collections of the relevant couplings. The mixing angle $\theta = -10.7°$ for η-η' mixing in the singlet-octet basis is reasonably adopted [61].

Couplings	Flavor symmetry
$g_{\kappa^0 K^+\pi^-} = 0.25 - 3.10i$ GeV [58]	$g_{SPP} = g_{\kappa^0 K^+\pi^-} = \sqrt{2} g_{\kappa^+ K^+\pi^0} = g_{\kappa^+ K^0\pi^+} = -\sqrt{2} g_{\kappa^0 K^0\pi^0}$
$g_{\kappa^0 K^0\eta} = -0.10 + 1.24i$ GeV	$g_{\kappa^0 K^0\eta} = g_{SPP} \frac{-1}{\sqrt{6}} \cos\theta$
$g'_{\kappa^0 K^0\eta} = -0.04 + 0.58i$ GeV	$g'_{\kappa^0 K^0\eta} = g_{SPP}[\frac{-1}{\sqrt{6}} \cos\theta + \frac{2}{\sqrt{3}}(-\sin\theta)]$
$g_{\sigma\pi^+\pi^-} = -0.79 + 2.84i$ GeV [56]	$2 g_{\sigma\pi^0\pi^0} = g_{\sigma\pi^+\pi^-} = 2 g_{\sigma K\bar{K}}$
$g_{\sigma K^0\bar{K}^0} = -0.39 + 1.42i$ GeV	$g_{\sigma K^+ K^-} = g_{\sigma K^0\bar{K}^0}$
$g_{\sigma\kappa^0\bar{\kappa}^0} = 3 g_{\sigma K^0\bar{K}^0} = -1.18 + 4.26i$ GeV	$g_{\sigma\kappa^+\kappa^-} = g_{\sigma\kappa^0\bar{\kappa}^0}$
$g_{\sigma\kappa^0\bar{K}^{*0}} = 3.27 - 0.25i$ GeV	$g_{\sigma\kappa^+ K^{*-}} = g_{\sigma\kappa^0\bar{K}^{*0}} = g_{VPP}/\sqrt{2}$
$g_{K^{*0}K^+\pi^-} = 4.63 - 0.35i$ [58]	$g_{VPP} = g_{K^{*0}K^+\pi^-}$
$g_{\rho^0\pi^+\pi^-} = -5.98 + 0.54i$ [56]	$\sqrt{2} g_{VPP} = g_{\rho^+\pi^+\pi^0} = -g_{\rho^-\pi^-\pi^0} = -g_{\rho^0\pi^+\pi^-}$
$g_{\rho^0 K^0\bar{K}^0} = 3.27 - 0.25i$	$g_{\rho^0 K^0\bar{K}^0} = g_{VPP}/\sqrt{2}$
$g_{\rho^0\kappa^0\bar{\kappa}^0} = g_{\rho^0 K^0\bar{K}^0} = 3.27 - 0.25i$	$g_{\rho^+\kappa^+\bar{\kappa}^0} = \sqrt{2} g_{\rho^0\kappa^+\kappa^-}$
$g_{\sigma\rho^+\rho^-} = g_{\sigma\pi^+\pi^-}$	$g_{\sigma\rho^+\rho^-} = \sqrt{2} g_{VVS}$
$g_{\rho^0\kappa^+ K^{*-}} = g_{VVS}/\sqrt{2} = -0.39 + 1.42i$ GeV	$g_{\rho^+\kappa^+\bar{K}^{*0}} = \sqrt{2} g_{\rho^0\kappa^+\bar{K}^{*-}}$, $g_{\rho^0\kappa^0\bar{K}^{*0}} = -g_{\rho^0\kappa^+ K^{*-}}$
$g_{SPP} = 0.25 - 3.10i$ GeV	
$g_{VPP} = 4.63 - 0.35i$ GeV	
$g_{VVS} = -0.55 + 2.01i$ GeV	

[a]Relations in the flavor symmetry column are derived from SU(3) symmetry. The numerical values of the couplings on the left side are extracted from different phenomenological analyses and therefore do not strictly satisfy these SU(3) relations. For instance, $g_{\rho^0\pi^+\pi^-}$ from Ref. [56] gives $g_{VPP} = 4.23 - 0.38i$, which slightly deviates from $g_{VPP} = g_{K^{*0}K^+\pi^-}$ from Ref. [58].

$\kappa^0\bar{\kappa}^0$ component is written as

$$i\mathcal{M}^N_{\pi^+\pi^-} = \int \frac{d^4 p_1}{(2\pi)^4} \frac{-g_{F\bar{\kappa}^0\kappa^0} \cdot g_{\bar{\kappa}^0 K^-\pi^+} \cdot g_{\kappa^0 K^+\pi^-}}{(p_1^2 - s_\kappa)(p_2^2 - m_K^2)(p_3^2 - s_\kappa)} \times \mathcal{F}(p_2^2, m_K^2). \tag{10}$$

Similarly, we can obtain the amplitude in this mechanism via the charged $\kappa^+\kappa^-$ component and denoted it as $\mathcal{M}^C_{\pi^+\pi^-}$. Notice that in the $\pi^+\pi^-$ channel no charge conjugated loop can contribute for both the neutral and charged κ components. The kinematic variables of the particles in the triangle loop are also denoted in Fig. 1(a). The effective Lagrangian approach, which deals with the nonlocal effects by introducing empirical form factors to cut off the divergences, is applied to broader kinematic regions. Hence, we include a commonly adopted monopole form factor to the exchanged mesons [62],

$$\mathcal{F}(p_{\rm ex}^2, m_{\rm ex}^2) = \frac{\Lambda^2 - m_{\rm ex}^2}{\Lambda^2 - p_{\rm ex}^2}, \tag{11}$$

where $\Lambda = m_{\rm ex} + \alpha\Lambda_{\rm QCD}$ with $\Lambda_{\rm QCD} = 300$ MeV, and α is a dimensionless cutoff parameter. $p_{\rm ex}$ and $m_{\rm ex}$ are the four-momentum and mass of the exchanged meson, respectively.

The physical meaning of the cutoff Λ is that it reflects the finite spatial size of the exchanged hadron. The monopole form factor with $\Lambda_{\rm QCD} \sim 300$ MeV was devised for typical $q\bar{q}$ mesons, whose size is governed by the quark-gluon confinement scale. For such narrow $q\bar{q}$ states (π, K, ρ, K^*, etc.), we reasonably choose $\alpha = 1, 2, 3$ in our calculation to examine the cutoff dependence.

However, for the wide scalar κ exchanged in the triangle loops, the physical picture is different: as molecular or non-$q\bar{q}$ states, they are loosely bound systems of constituent hadrons rather than compact quark-gluon bound states. Their spatial extension is governed by hadronic binding scales, which are softer than the quark confinement scale. Consequently, a lower cutoff is physically appropriate for these states. In the absence of a well-established form factor prescription for wide molecular states, we adopt a simple prescription: for the exchanged κ, we shift the cutoff parameter downward by roughly 0.5–1 compared to that for ordinary $q\bar{q}$ mesons. Specifically, we use $\alpha_B = 0.5, 1, 2$ as the cutoff parameters for the exchanged wide scalars, respectively, corresponding to the $\alpha = 1, 2, 3$ for the narrow $q\bar{q}$ states. However, due to the lack of knowledge about the behavior of the counter terms, yet another model dependence will be present in association with the cutoff energies and different forms for the form factors [63].

Based on the flavor symmetry, we have $g_{\kappa^0 K^+\pi^-} = g_{\kappa^+ K^0\pi^+} = \sqrt{2} g_{\kappa^+ K^+\pi^0} = -\sqrt{2} g_{\kappa^0 K^0\pi^0}$. In the isospin symmetry limit, the total partial width of the $\pi\pi$ channel is calculated by

$$\Gamma_{\pi\pi} = \frac{3}{2} \times \frac{1}{2m_F} \int d\Phi_{\pi\pi} |\mathcal{M}^N_{\pi^+\pi^-} + \mathcal{M}^C_{\pi^+\pi^-}|^2, \tag{12}$$

where $\Phi_{\pi\pi}$ indicate the $\pi\pi$ phase space. The factor $3/2$ originates from the inclusion of the $\pi^0\pi^0$ final state

considering their identical feature and the relations in couplings.

The mechanism for the $f_0(1370)$ decay to $\eta\eta$ is the same as that for decay to $\pi^+\pi^-$, where one is just changing the vertices of $\kappa \to K\pi$ to $\kappa \to K\eta$. Hence, by replacing these couplings we can obtain the amplitudes $\mathcal{M}^C_{\eta\eta}$ and $\mathcal{M}^N_{\eta\eta}$ for the $\eta\eta$ final states. Note that the charge conjugated loop can contribute for both the neutral and charged κ components in this channel. The decay width of the $\eta\eta$ channel is given by

$$\Gamma_{\eta\eta} = \frac{1}{2} \times \frac{1}{2m_F} \int d\Phi_{\eta\eta} |2\mathcal{M}^N_{\eta\eta} + 2\mathcal{M}^C_{\eta\eta}|^2, \quad (13)$$

$\Phi_{\eta\eta}$ is the phase space of $\eta\eta$ final states and $1/2$ is the symmetry factor.

The coupling $g_{\kappa K\eta}$ can be related to $g_{\kappa^0 K^+\pi^-}$ by the flavor symmetry. In fact, the physical η state is the mixing of η_8 and η_1 with $\eta = \cos\theta\eta_8 - \sin\theta\eta_1$ due to the SU(3) flavor breaking. As shown in Table I, we adopt two strategies to deal with the $g_{\kappa K\eta}$ coupling: one is that we ignore the η_1 component in η by taking $\eta = \cos\theta\eta_8$, and restrict to the symmetry inside the octet by using P_8 as the pseudoscalar matrix. In this case, we denote this coupling as $g_{\kappa K\eta}$; the other case is that we take $\eta = \cos\theta\eta_8 - \sin\theta\eta_1$ and relate the couplings associated with these two parts as well as the $g_{\kappa K\pi}$ by the U(3) flavor symmetry, where the pseudoscalar matrix is taken as U. In this case, this coupling is denoted as $g'_{\kappa K\eta}$. The explicit forms of P_8 and U can be found in Appendix. C. One must account for the fact that the $U(3)$ flavor symmetry is not good enough in the pseudoscalar sector due to the U(1) anomaly.

Similarly, as shown in Fig. 1(b), the amplitude of $f_0(1370)$ decay to K^+K^- channel by exchanging π via the neutral $\kappa^0\bar{\kappa}^0$ component is written as

$$i\mathcal{M}^N_{K^+K^-} = \int \frac{d^4p_1}{(2\pi)^4} \frac{-g_{F\bar{\kappa}^0\kappa^0} \cdot g_{\bar{\kappa}^0 K^-\pi^+} \cdot g_{\kappa^0 K^+\pi^-}}{(p_1^2 - s_\kappa)(p_2^2 - m_\pi^2)(p_3^2 - s_\kappa)} \times \mathcal{F}(p_2^2, m_\pi^2). \quad (14)$$

Same as the case in $\pi\pi$ channel, there is no charge conjugated loop that can contribute. Considering the relation between the couplings $g_{\kappa^0 K^+\pi^-}$ and $g_{\kappa^+ K^+\pi^0}$, we find that $\mathcal{M}^C_{K^+K^-} = (1/2)\mathcal{M}^N_{K^+K^-}$. The amplitude of $f_0(1370)$ decay to K^+K^- channel by exchanging η is written as

$$i\mathcal{M}'_{K^+K^-} = \int \frac{d^4p_1}{(2\pi)^4} \frac{-g_{F\kappa^+\kappa^-} \cdot g_{\kappa^+K^+\eta} \cdot g_{\kappa^-K^-\eta}}{(p_1^2 - s_\kappa)(p_2^2 - m_\eta^2)(p_3^2 - s_\kappa)} \times \mathcal{F}(p_2^2, m_\eta^2). \quad (15)$$

Then we obtain the total decay width to $K\bar{K}$ via

$$\Gamma_{K\bar{K}} = 2 \times \frac{1}{2m_F} \int d\Phi_{K\bar{K}} |\mathcal{M}^N_{K^+K^-} + \mathcal{M}^C_{K^+K^-} + \mathcal{M}'_{K^+K^-}|^2, \quad (16)$$

where the $\Phi_{K\bar{K}}$ indicate the $K\bar{K}$ phase space. The factor 2 originates from the inclusion of $K^0\bar{K}^0$ final state.

For the 4π decay channel, there are three different specific final states that are $2\pi^+2\pi^-$, $\pi^+\pi^-2\pi^0$, and $4\pi^0$, respectively. As claimed by the analyses in experiments [20,23,24], the 4π final states are mainly from the intermediate channels of $\sigma\sigma$ and $\rho\rho$. This mechanism is shown in Fig. 1(c). Specifically, for the decay of an isoscalar state f_0, the $2\pi^+2\pi^-$ channel is only from the $\rho^0\rho^0$ and $\sigma\sigma$ intermediate channels; the $\pi^+\pi^-2\pi^0$ channel is only from the $\rho^+\rho^-$ and $\sigma\sigma$ intermediate channels; and the $4\pi^0$ channel is only from the $\sigma\sigma$ intermediate channel. Because these final states include identical particles, we must account for additional contributions arising from identical particles exchange.

Firstly we focus on the decay width of the $2\pi^+2\pi^-$ channel, then the decay widths of the other two channels can be related to $\Gamma_{2\pi^+2\pi^-}$ by considering the relations among the couplings in the isospin limit. As shown in Fig. 1(c), we consider the decay mechanism of $\kappa\bar{\kappa}$ rescattering to $\rho\rho$ or $\sigma\sigma$ first and subsequently decaying to 4π. The amplitude of the process for $\kappa\bar{\kappa}$ rescattering to $2\sigma \to 2\pi^+2\pi^-$ by exchanging scalar κ, denoted as $\mathcal{M}^S_\sigma$, has the form of,

$$i\mathcal{M}^S_\sigma = 4 \int \frac{d^4p_1}{(2\pi)^4} \frac{-g_{F\kappa^0\bar{\kappa}^0} \cdot g^2_{\sigma\kappa^0\bar{\kappa}^0} \cdot g^2_{\sigma\pi^+\pi^-} \mathcal{F}(p_2^2, m_\kappa^2)}{(p_1^2 - s_\kappa)(p_2^2 - s_\kappa)(p_3^2 - s_\kappa)(p_{ab}^2 - s_\sigma)(p_{cd}^2 - s_\sigma)} + ex., \quad (17)$$

momenta of the final π are denoted as $\pi^+(p_a)\pi^-(p_b)\pi^+(p_c)\pi^-(p_d)$, and $p_{ab} = p_a + p_b$, $p_{cd} = p_c + p_d$ are, respectively, the momenta of the two intermediate σ. The $ex.$ term indicates the contribution from exchanging the identical particles, which is the same as the first term but only change the momenta of the two σ to $p_{ad} = p_a + p_d$ and $p_{bc} = p_b + p_c$, respectively. Note that, for such a decay mechanism, there are two charge conjugated loops for both the charged and neutral $\kappa\bar{\kappa}$ rescattering. By analyzing the relations of the couplings involved, we find that the amplitudes of these four diagrams are identical, resulting in a multiplicative factor of 4.

Similarly, the amplitude of the process shown in Fig. 1(c) for the $\kappa\bar{\kappa}$ rescattering to $2\sigma \to 2\pi^+2\pi^-$ by exchanging

vector K^*, denoted as $\mathcal{M}^V_\sigma$, has the form of

$$i\mathcal{M}^V_\sigma = 4\times G\int\frac{d^4p_1}{(2\pi)^4}\frac{(p_{ab}+p_1)_\mu(p_{cd}+p_3)_\nu\left(g^{\mu\nu}-\frac{p_2^\mu p_2^\nu}{m^2_{K^*}}\right)\mathcal{F}(p_2^2,m^2_{K^*})}{(p_1^2-s_\kappa)(p_2^2-m^2_{K^*})(p_3^2-s_\kappa)(p^2_{ab}-s_\sigma)(p^2_{cd}-s_\sigma)}+\text{ex.}, \tag{18}$$

here for brevity we use $G=g_{F\kappa^0\bar\kappa^0}\cdot g^2_{\sigma\kappa^0\bar K^{*0}}\cdot g^2_{\sigma\pi^+\pi^-}$.

The amplitude of the process for the $\kappa\bar\kappa$ rescattering to $2\rho^0\to 2\pi^+2\pi^-$ by exchanging κ, as shown in Fig. 1(c), has the form of

$$i\mathcal{M}^S_\rho = 4\times G\int\frac{d^4p_1}{(2\pi)^4}\frac{(p_1+p_2)_\mu(p_3-p_2)_\alpha\left(g^{\mu\nu}-\frac{p^\mu_{ab}p^\nu_{ab}}{m^2_\rho}\right)\left(g^{\alpha\beta}-\frac{p^\alpha_{cd}p^\beta_{cd}}{m^2_\rho}\right)(p_a-p_b)_\nu(p_c-p_d)_\beta\mathcal{F}(p_2^2,m^2_K)}{(p_1^2-s_\kappa)(p_2^2-s_\kappa)(p_3^2-s_\kappa)(p^2_{ab}-m^2_\rho+im_\rho\Gamma_\rho)(p^2_{cd}-m^2_\rho+im_\rho\Gamma_\rho)}+\text{ex.}, \tag{19}$$

here $G=g_{F\kappa^0\bar\kappa^0}\cdot g^2_{\rho^0\kappa^0\bar\kappa^0}\cdot g^2_{\rho^0\pi^+\pi^-}$.

The amplitude of the process for the $\kappa\bar\kappa$ rescattering to $2\rho^0\to 2\pi^+2\pi^-$ by exchanging K^*, as shown in Fig. 1(c), has the form of

$$i\mathcal{M}^V_\rho = 4\times G\int\frac{d^4p_1}{(2\pi)^4}\frac{\left(g_{\mu\alpha}-\frac{p_{2\mu}p_{2\alpha}}{m^2_{K^*}}\right)\left(g^{\mu\nu}-\frac{p^\mu_{ab}p^\nu_{ab}}{m^2_\rho}\right)\left(g^{\alpha\beta}-\frac{p^\alpha_{cd}p^\beta_{cd}}{m^2_\rho}\right)(p_a-p_b)_\nu(p_c-p_d)_\beta\mathcal{F}(p_2^2,m^2_{K^*})}{(p_1^2-s_\kappa)(p_2^2-m^2_{K^*})(p_3^2-s_\kappa)(p^2_{ab}-m^2_\rho+im_\rho\Gamma_\rho)(p^2_{cd}-m^2_\rho+im_\rho\Gamma_\rho)}+\text{ex.}, \tag{20}$$

here $G=g_{F\kappa^0\bar\kappa^0}\cdot g^2_{\rho^0\kappa^0\bar K^{*0}}\cdot g^2_{\rho^0\pi^+\pi^-}$. The total amplitude of decaying to $2\pi^+2\pi^-$ is the sum of all the amplitudes above, i.e.,

$$\mathcal{M}_{2\pi^+2\pi^-}=\mathcal{M}^S_\sigma+\mathcal{M}^V_\sigma+\mathcal{M}^S_\rho+\mathcal{M}^V_\rho. \tag{21}$$

The decay width of this final state is

$$\Gamma_{2\pi^+2\pi^-}=\frac{1}{4}\cdot\frac{1}{2m_F}\int d\Phi_{2\pi^+2\pi^-}|\mathcal{M}_{2\pi^+2\pi^-}|^2. \tag{22}$$

The constant $1/4$ is the symmetry factor on account of the two kinds of identical particles: two π^+ and two π^-.

Then, we can discuss the decay amplitudes of $\pi^+\pi^-2\pi^0$ and $4\pi^0$ states based on the amplitude of the $2\pi^+2\pi^-$ state. For the $\rho^+\rho^-\to\pi^+(p_a)\pi^0(p_b)-\pi^-(p_c)\pi^0(p_d)$ process, we find the following similarities and differences compared to the $\rho^0\rho^0\to\pi^+(p_a)\pi^-(p_b)-\pi^+(p_c)\pi^-(p_d)$:

(i) There is no charge conjugated loop for both the charged and neutral $\kappa\bar\kappa$ rescattering.
(ii) Comparison of the relations between couplings $g_{\rho^+\kappa\bar\kappa}/g_{\rho^+\kappa\bar K^*}$ and $g_{\rho^0\kappa\bar\kappa}/g_{\rho^0\kappa\bar K^*}$ shown in Table I.
(iii) Including the diagram obtained from exchanging the two identical π^0.
(iv) The relation of the coupling $g_{\rho^\pm\pi^\pm\pi^0}$ and $g_{\rho^0\pi^+\pi^-}$ shown in Table I.

Considering the above items we find that the amplitudes adapted to the $\rho^+\rho^-\to\pi^+\pi^-2\pi^0$ process are just $-\mathcal{M}^S_\rho$ and $-\mathcal{M}^V_\rho$.

For the $\sigma\sigma\to\pi^+(p_a)\pi^-(p_c)-\pi^0(p_b)\pi^0(p_d)$ process, we find the following discrepancies compared to the $\sigma\sigma\to\pi^+(p_a)\pi^-(p_b)-\pi^+(p_c)\pi^-(p_d)$:

(i) The exchange of the two identical π^0 from the same σ is topologically identical.
(ii) The relation of couplings: $g_{\sigma\pi^+\pi^-}=2g_{\sigma\pi^0\pi^0}$.
(iii) There are two ways to contract the two π^0 fields and the two final π^0 states at the $\sigma\pi^0\pi^0$ vertex.

Therefore, the amplitudes $\mathcal{M}^S_\sigma$ and $\mathcal{M}^V_\sigma$ adapted to the $\pi^+\pi^-2\pi^0$ state are obtained by changing the momenta of the two σ to $p_{ac}=p_a+p_c$ and $p_{bd}=p_b+p_d$, respectively, and eliminating the exchange terms.

The decay width of the $\pi^+\pi^-2\pi^0$ state is

$$\Gamma_{\pi^+\pi^-2\pi^0}=\frac{1}{2}\cdot\frac{1}{2m_F}\int d\Phi_{\pi^+\pi^-2\pi^0}|\mathcal{M}_{\pi^+\pi^-2\pi^0}|^2. \tag{23}$$

The constant $1/2$ is the symmetry factor on account of the two identical particles π^0.

For the $\sigma\sigma\to 4\pi^0$ process, the amplitudes $\mathcal{M}^S_\sigma$ and $\mathcal{M}^V_\sigma$ for $2\pi^+2\pi^-$ can be adopted directly, but all possible exchanges of the π^0 must be further included. The decay width of the $4\pi^0$ state is

$$\Gamma_{4\pi^0}=\frac{1}{4!}\cdot\frac{1}{2m_F}\int d\Phi_{4\pi^0}|\mathcal{M}_{4\pi^0}|^2. \tag{24}$$

The constant $1/4!$ is the symmetry factor on account of the four identical particles π^0.

For the $K\bar{K}\pi\pi$ channel from the tree-level decay $f_0(1370) \to \kappa\bar{\kappa} \to (K\pi)(\bar{K}\pi)$ shown in Fig. 1(d), there are six different final states specifically. The $K^+K^-\pi^+\pi^-$ and $K^0\bar{K}^0\pi^0\pi^0$ can only originate from the $\kappa^0\bar{\kappa}^0$ component; the $K^0\bar{K}^0\pi^+\pi^-$ and $K^+K^-\pi^0\pi^0$ can only originate from the $\kappa^+\kappa^-$ component; while the $K^0K^-\pi^+\pi^0$ and $K^+\bar{K}^0\pi^0\pi^-$ can originate from both the $\kappa^0\bar{\kappa}^0$ and $\kappa^+\kappa^-$ components.

For the $K^+K^-\pi^+\pi^+$ final state, the amplitude is:

$$\mathcal{M}_{K^+K^-\pi^+\pi^-} = g_{F\kappa^0\bar{\kappa}^0} \cdot g^2_{\kappa^0 K^+\pi^-} G_\kappa(s_{ab}) G_{\bar{\kappa}}(s_{cd}), \qquad (25)$$

where s_{ab} and s_{cd} are, respectively, the invariant mass squares of the $K\pi$ pairs coming from κ and $\bar{\kappa}$. The amplitudes of other final states can be obtained by replacing the couplings in $\mathcal{M}_{K^+K^-\pi^+\pi^-}$ and carefully including all the possible diagrams. The combinations of $K\pi$ are definite for all the $K\bar{K}\pi\pi$ channels except for $K^+K^-\pi^0\pi^0$ and $K^0\bar{K}^0\pi^0\pi^0$ due to the two identical particles π^0. Hence, for these two final states, we need to include another diagram obtained by exchanging these two π^0 and when calculating the decay width, the symmetry factor $1/2$ should be considered on account of the double counting in the phase space.

Moreover, we address the implications of the SU(3) flavor symmetry for the scalar-scalar molecular picture adopted here. If $f_0(1370)$ is a $\kappa\bar{\kappa}$ molecule, the flavor symmetry seems to imply the existence of a full molecular multiplet. To study this issue, we have performed a systematic analysis of the vector-exchange induced effective potentials between scalar-meson pairs based on the $\mathcal{L}_{SSV}$ Lagrangian, Eq. (7). For a given channel, the t- and u-channel potentials are evaluated at threshold via $V_{\rm eff} = \sum_V g_a^{(V)} g_b^{(V)} / m_V^2$, where $g_a^{(V)}$ and $g_b^{(V)}$ are, respectively, the couplings of the upper and lower vertices that exchange vector V. Then the effective potential $V^I_{\rm eff}$ with specific isospin is obtained by projecting the total potentials onto states of fixed total isospin using the convention adopted here.

For simplicity, we set the overall coupling $g_{SSV} = 1$, the quantity $V^I_{\rm eff}$ should therefore be interpreted as relative indicators for comparing attraction or repulsion strengths across different channels, rather than as absolute potential strengths. The resulting effective potentials (in units of GeV^{-2}) are summarized in Table II.

The $\kappa\bar{\kappa}$ channel in $I = 0$ receives attractive contributions from ω, ρ^0, ϕ, and $\rho^\pm$ exchange, providing independent support for the $\kappa\bar{\kappa}$ molecular interpretation of $f_0(1370)$. The vanishing of a_0a_0 in $I = 1$ follows exactly from the antisymmetry of the scattering amplitude. Among the mixed channels, only $a_0\kappa$ in $I = 1/2$ is attractive, driven by off-diagonal $\rho^\pm$ exchange. It is noteworthy that this pattern of attraction is analogous to the pseudoscalar-meson sector, where scalar resonances are only observed in $\pi\pi$ ($I = 0$), $K\pi$ ($I = 1/2$), and $K\bar{K}$ ($I = 0$, 1). The a_0a_0 $I = 0$ molecule might be assigned to the $f_0(2020)/f_0(2100)/f_0(2200)$ listed in the RPP, and the $a_0\kappa I = 1/2$ molecule might be assigned to the $K_0^*(1430)/K_0^*(1950)$. We note that this analysis is restricted to vector-meson exchange, which is expected to be the dominant mechanism; other possible contributions are not considered here.

TABLE II. Effective potentials $V^I_{\rm eff}$ for scalar-meson pair channels from t- and u-channel vector-meson exchange, evaluated with $g_{SSV} = 1$.

Channel	Isospin	$V^I_{\rm eff}$ (GeV^{-2})
$\kappa\bar{\kappa}$	$I = 0$	−4.27 (Strongly attractive)
$\kappa\bar{\kappa}$	$I = 1$	−0.95 (Weakly attractive)
a_0a_0	$I = 0$	−13.3 (Strongly attractive)
a_0a_0	$I = 1$	0 (Exact cancellation)
a_0a_0	$I = 2$	+6.66 (Repulsive)
$\sigma\sigma$, σa_0, σf_0, f_0f_0, a_0f_0	$I = 0/1$	0 (Forbidden)
$a_0\kappa$	$I = 1/2$	−3.19 (Attractive)
$a_0\kappa$	$I = 3/2$	+2.92 (Repulsive)
$f_0\kappa$	$I = 1/2$	+1.26 (Repulsive)
$\sigma\kappa$	$I = 1/2$	+0.63 (Repulsive)

III. NUMERICAL RESULTS AND DISCUSSIONS

The partial decay widths of different channels we calculated including $K\bar{K}$, $\pi\pi$, $\eta\eta$, 4π, and $K\bar{K}\pi\pi$, these are the primary strong decay channels of $f_0(1370)$, which are approximately summed up to the total width of $f_0(1370)$: the Γ_F. We first present the total width at $\sqrt{s} = 1.37$ GeV with $g_{F\kappa\bar{\kappa}}$ treated as a free parameter in Fig. 2. We take this couplings as a parameter to fit the total width of $f_0(1370)$ measured in experiments. We will present results for two different couplings $g_{\kappa K\eta}$ and $g'_{\kappa K\eta}$ in this section.

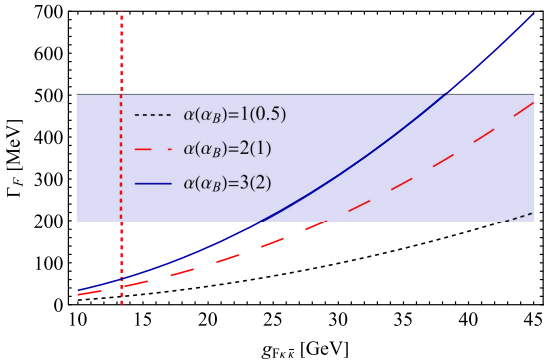


FIG. 2. Total width of $f_0(1370)$ dependent on the parameter $g_{F\kappa\bar{\kappa}}$ with $\sqrt{s} = 1.37$ GeV and three form factor parameter sets $\alpha(\alpha_B) = 1(0.5)/2(1)/3(2)$. The red dashed vertical line indicates the reference value $g_{F\kappa\bar{\kappa}} = 13.4$ GeV which is estimated from the Weinberg compositeness criterion [64,65] using a complex κ mass $\sqrt{s_\kappa} = 0.7 - 0.3i$ GeV with $X = 1$; the light purple band indicates the range of the Breit-Wigner width of $f_0(1370)$ measured in experiments.

For clarity, we denote the result associated with $g_{\kappa K\eta}$ as Γ_F and with $g'_{\kappa K\eta}$ as Γ'_F. We approximate the total 4π width by summing the $\sigma\sigma$ and $\rho\rho$ contributions, under the assumption that other intermediate states are negligible. In our framework, the $f_0(1370)$ decaying to the $K\bar{K}, \pi\pi, \eta\eta$, and 4π channels are via the triangle loop diagrams, which are dependent on the cutoff parameters α. Hence, we also present the results with different cutoff parameters $\alpha(\alpha_B)$ from $1(0.5) \sim 3(2)$ in Fig. 2, to study the cutoff dependence. The light purple band in Fig. 2 indicates the range of the Breit-Wigner width of $f_0(1370)$ measured in experiments. The pole width $\Gamma = -2\,\mathrm{Im}\sqrt{s_{\mathrm{pole}}}$ for $f_0(1370)$ is estimated to be around 500 MeV according to its pole position, and its Breit-Wigner width is measured to be between 200 MeV and 500 MeV depending on the models and the reactions. The red dashed vertical line indicates the reference value $g_{F\kappa\bar{\kappa}} = 13.4$ GeV, as estimated from the Weinberg criterion [64,65] using a complex κ mass $\sqrt{s_\kappa} = 0.7 - 0.3i$ GeV and compositeness $X = 1$. As shown in Fig 2, with the $g_{F\kappa\bar{\kappa}}$ determined by the Weinberg criterion, the total width Γ_F is much smaller than the measured values of $f_0(1370)$ collected in the RPP [8]. It is expected that the Weinberg criterion does not work for our broad component case even if a complex mass is used because it is derived from the situation of weakly bound state consisting of two stable or nearly stable components.

From Fig. 2 we can see that when cutoff parameter $\alpha(\alpha_B) = 1(0.5)$, the coupling $g_{F\kappa\bar{\kappa}}$ is taken as large as 45 GeV, the total width Γ_F could merely reach the lower limit of the experimental width range. While with $\alpha(\alpha_B) = 2(1)$, Γ_F can reach the experimental observation when $g_{F\kappa\bar{\kappa}}$ is around 30 GeV. Certainly with $\alpha(\alpha_B) = 3(2)$, the required $g_{F\kappa\bar{\kappa}}$ to reproduce the experimental width is further reduced to about 25 GeV. For presenting the accurate quantities of the partial widths of different channels when the total width is fitted to experiments, we show the results in Table III with $g_{F\kappa\bar{\kappa}} = 35$ GeV. Notice that $g_{F\kappa\bar{\kappa}}$ is a common coupling for all the decay channels, its change will not affect the ratios among the decay channels. In other words, the decay pattern is independent of this coupling.

From Table III, we can see that when $\alpha(\alpha_B)$ varies from 2(1) to 3(2), the decay widths are relatively stable. These decay channels have been observed in experiments except the $K\bar{K}\pi\pi$ channel, which lacks measurements up to now. At the nominal mass of $f_0(1370)$: $\sqrt{s} = 1.37$ GeV, the $K\bar{K}$ channel has the largest partial width, followed by the 4π and $\pi\pi$ channels. The $\pi\pi$ and 4π channels have comparable partial widths. We can find that the partial width of $K\bar{K}$ channel is not sensitive to the strategy that determining the $\kappa K\eta$ coupling because the most dominant contribution to this channel is the mechanism of exchanging π.

From Table I, we find that the U(3) symmetry expression of the $g'_{\kappa K\eta}$ coupling consists of two destructive terms, which, respectively, correspond to the η_8 and η_1 parts in the mixing wave function. We adopt a relatively large value of $\theta = -10.7°$ referring to the analysis in [59,61]. Due to the comparable size of these two parts, the destructive interference leads to a small value of $g'_{\kappa K\eta}$, which is sensitive to the mixing angle θ. Hence, the partial width $\Gamma'(F \to \eta\eta)$ calculated with $g'_{\kappa K\eta}$ is the smallest, with its order of magnitude being one-thousandth of the partial widths of the other channels. Compared to it, $\Gamma(F \to \eta\eta)$ is larger by a factor of about 20 because the coupling $g_{\kappa K\eta}$ is not suppressed by the destructive interference. But $g_{\kappa K\eta}$ is still smaller than $g_{\kappa K\pi}$, which is contrary to the relation between $g_{K^*K\pi}$ and $g_{K^*K\eta}$: $g_{K^*K\pi^\pm} : g_{K^*K\eta} = 1 : (\sqrt{3}/\sqrt{2})\cos\theta$, because the irreducible decomposition of $8 \otimes 8$ includes two different octet 8_A and 8_S. Here A and S indicate the antisymmetric and symmetric features corresponding to the K^* and κ flavor wave functions, respectively, which leads to different coupling relations. Therefore, the calculations treating the $f_0(1710)$ as a $K^*\bar{K}^*$ molecular state in Ref. [66] show that its decays into $\eta\eta$ and $\pi\pi$ channels are in the same order of magnitude. While with the same triangle diagram mechanism exchanging K, the partial widths of $f_0(1370)$ treated as a $\kappa\bar{\kappa}$ molecule to these two channels differ by one to two orders of magnitude.

The $K\bar{K}\pi\pi$ channel is the only one proceeding through tree-level decay. However, the partial width of this channel is much smaller than that of the $K\bar{K}$, $\pi\pi$, and 4π channels, which arise from loop-level decays. This phenomenon might be mainly attributed to the very limited $K\bar{K}\pi\pi$ phase space compared to the other channels around $\sqrt{s} = 1.37$ GeV, which is near the $\kappa\bar{\kappa}$ threshold.

TABLE III. Partial widths of different channels in $f_0(1370)$ decay at fixed $\sqrt{s} = 1.37$ GeV, with $g_{F\kappa\bar{\kappa}} = 35.0$ GeV. For testing the cutoff dependence, the cutoff parameter for the loop diagrams is chosen as $\alpha(\alpha_B) = 1(0.5)/\mathbf{2(1)}/3(2)$ for $K^*(\kappa)$ exchange. Γ_F is the sum of all the partial decay widths listed here, which can be approximately taken as the total width of $f_0(1370)$. We present results for two different couplings $g_{\kappa K\eta}$ and $g'_{\kappa K\eta}$ and denote the result associated with $g'_{\kappa K\eta}$ as Γ'. The decay widths are presented in units of MeV. Boldface values correspond to the reference cutoff choice $\alpha(\alpha_B) = 2(1)$. The single $K\bar{K}\pi\pi$ entry is independent of the loop cutoff.

Decay channel	$g_{F\kappa\kappa} = 35.0$ GeV
$\Gamma(F \to K\bar{K})$	$47.5/\mathbf{132}/207$
$\Gamma'(F \to K\bar{K})$	$43.5/\mathbf{121}/189$
$\Gamma(F \to \pi\pi)$	$22.1/\mathbf{62.7}/103$
$\Gamma(F \to \eta\eta)$	$0.72/\mathbf{1.94}/3.08$
$\Gamma'(F \to \eta\eta)$	$3.3 \times 10^{-2}/\mathbf{9} \times \mathbf{10^{-2}}/0.14$
$\Gamma(F \to 4\pi)$	$61.7/\mathbf{92.6}/105.0$
$\Gamma(F \to K\bar{K}\pi\pi)$	**0.33**
Γ_F	$134/\mathbf{291}/420$
Γ'_F	$129/\mathbf{278}/400$

Consequently, around this energy region, the $K\bar{K}\pi\pi$ width is sensitive to the center-of-mass energy $\sqrt{s}$.

With $g_{F\kappa\bar{\kappa}} = 35$ GeV, the partial widths of different specific $K\bar{K}\pi\pi$ final states at $\sqrt{s} = 1.37$ GeV are as follows: $\Gamma(K^+K^-\pi^+\pi^-) = \Gamma(K^0\bar{K}^0\pi^+\pi^-) = 108$ keV; $\Gamma(K^+K^-\pi^0\pi^0) = \Gamma(K^0\bar{K}^0\pi^0\pi^0) = 54$ keV; $\Gamma(K^+\bar{K}^0\pi^0\pi^-) = \Gamma(K^0K^-\pi^+\pi^0) = 0.53$ keV. For the states with two charged π, the charged couplings $g_{\kappa K\pi^\pm}$ is larger than the neutral couplings by a factor of $\sqrt{2}$. While for the states including $\pi^0\pi^0$, there are another exchanged diagram and an extra symmetry factor $1/2$, finally leading to such a relation. For the states including only one charged pion, there are two diagrams respectively from the two different $\kappa\bar{\kappa}$ components, which interfere destructively due to the $SU(3)$ relations listed in Table I, resulting in a very small partial width for these states. Such a pattern is different from the direct decay to $K\bar{K}\pi\pi$, such as the data in J/ψ decay [8]. The same decay pattern among these three kinds of $K\bar{K}\pi\pi$ states should also appear in the $K^*\bar{K}^* \to (K\pi)(\bar{K}\pi)$ process due to the same relations of couplings in $K^*K\pi$ and $\kappa K\pi$.

It is worth mentioning that in our framework, the decay widths to $K\bar{K}$, $\pi\pi$, $\eta\eta$, and $K\bar{K}\pi\pi$ are sensitive to the coupling $g_{\kappa K\pi}$ because they are essentially proportional to the fourth power of this coupling. In fact, the $|\tilde{g}_{\kappa K\pi}|$ is determined to be 4.4 [67] and 3.81 [58] in two different works, respectively, while such a small difference in this coupling can lead to a variation in these partial widths by nearly a factor of two.

The partial widths of different specific 4π final states at $\sqrt{s} = 1.37$ GeV are shown in Table IV, where we also present the exclusive contributions from different diagrams and intermediate states. The ratios between different 4π states are closely related to the decay mechanisms, as the intermediate states $\rho\rho$ and $\sigma\sigma$ have distinct features in 4π decay. These differences can reflect the decay dynamics of the $f_0(1370)$ and thereby reveal its structure. Reviewing the respective amplitudes for $2\pi^+2\pi^-$ and $\pi^+\pi^-2\pi^0$ as well as the results at $\sqrt{s} = 1.37$ GeV presented in Table IV, we find that in our framework, the contributions from the $\sigma\sigma \to 2\pi^+2\pi^-$ are much larger than those from $\rho^0\rho^0 \to 2\pi^+2\pi^-$. The width of the process $\sigma\sigma \to \pi^+\pi^-2\pi^0$ is smaller than that of $\sigma\sigma \to 2\pi^+2\pi^-$ even though the symmetry factor for $\pi^+\pi^-2\pi^0$ is larger. This is mainly because there is no identical particle exchange diagram in the $\sigma\sigma \to \pi^+\pi^-2\pi^0$ process where the two π^0 are from the same σ. In contrast, the process $\sigma\sigma \to 2\pi^+2\pi^-$ does include the contributions from such an exchange diagram. After the analysis it is found that the amplitudes for $\rho\rho$ decay to $2\pi^+2\pi^-$ and $\pi^+\pi^-2\pi^0$ are the same, then their widths only differ by the symmetry factor, which brings the relation of $2\Gamma(\rho\rho \to 2\pi^+2\pi^-) = \Gamma(\rho\rho \to \pi^+\pi^-2\pi^0)$ as listed in Table IV.

Hence, if the structure of $f_0(1370)$ is more likely to decay via the $\sigma\sigma$ intermediate state, the width of the $2\pi^+2\pi^-$ channel will be approximately twice that of the $\pi^+\pi^-2\pi^0$ channel. In contrast, if the $\rho\rho$ intermediate state dominates, the width of the $\pi^+\pi^-2\pi^0$ will be almost twice that of the $2\pi^+2\pi^-$ channel. Including both types of

TABLE IV. Decay widths of $f_0(1370) \to 4\pi$ with $g_{F\kappa\bar{\kappa}} = 35$ GeV. Exclusive widths for each diagram and different intermediate channels are also presented. The notation [ex, $R \to ff$] in the second column specifies the exchange particle "ex" between the κ pair and the intermediate resonance "R" decaying to final states "ff." The decay widths are given in three different choices of the cutoff parameters $\alpha(\alpha_B) = 1(0.5)/2(1)/3(2)$. Decay widths are evaluated at center-of-mass energy $\sqrt{s} = 1.37$ GeV and given in units of MeV. Boldface entries denote the coherent sums over the relevant exchange mechanisms and the resulting total widths; nonbold entries denote exclusive contributions from individual diagrams.

Channels	Diagram	$\sqrt{s} = 1.37$ GeV	The relevant couplings
$2\pi^+2\pi^-$	$[\kappa, \sigma \to \pi^+\pi^-]$	$\Gamma_1 = 6.5/8.5/14.6$	$g_{\sigma\kappa\bar{\kappa}}$, $g_{\sigma\pi^+\pi^-}$
	$[K^*, \sigma \to \pi^+\pi^-]$	$\Gamma_2 = 16.7/47.6/101$	$g_{\sigma\kappa\bar{K}^*}$, $g_{\sigma\pi^+\pi^-}$
	$\sigma\sigma \to 2\pi^+2\pi^-$	**30.9/46.1/49.9**	
	$[\kappa, \rho^0 \to \pi^+\pi^-]$	$\Gamma_3 = 0.24/1.00/3.86$	$g_{\rho^0\kappa\bar{\kappa}}$, $g_{\rho^0\pi^+\pi^-}$
	$[K^*, \rho^0 \to \pi^+\pi^-]$	$\Gamma_4 = 0.10/0.29/0.52$	$g_{\rho^0\kappa\bar{K}^*}$, $g_{\rho^0\pi^+\pi^-}$
	$\rho\rho \to 2\pi^+2\pi^-$	**0.33/1.20/3.97**	
	Total	**31.6/47.4/52.6**	
$\pi^+\pi^-2\pi^0$	$[\kappa, \sigma \to \pi^+\pi^-/\sigma \to \pi^0\pi^0]$	3.98/5.18/8.90	$g_{\sigma\kappa\bar{\kappa}}$, $g_{\sigma\pi^+\pi^-}$, $g_{\sigma\pi^0\pi^0}$
	$[K^*, \sigma \to \pi^+\pi^-/\sigma \to \pi^0\pi^0]$	9.67/27.8/59.7	$g_{\sigma\kappa\bar{K}^*}$, $g_{\sigma\pi^+\pi^-}$, $g_{\sigma\pi^0\pi^0}$
	$\sigma\sigma \to \pi^+\pi^-2\pi^0$	**18.0/26.1/27.9**	
	$[\kappa, \rho^+ \to \pi^+\pi^0/\rho^- \to \pi^-\pi^0]$	$2\Gamma_3$	$g_{\rho^\pm\kappa\bar{\kappa}}$, $g_{\rho^\pm\pi^\pm\pi^0}$
	$[K^*, \rho^+ \to \pi^+\pi^0/\rho^- \to \pi^-\pi^0]$	$2\Gamma_4$	$g_{\rho^\pm\kappa\bar{K}^*}$, $g_{\rho^\pm\pi^\pm\pi^0}$
	$\rho\rho \to \pi^+\pi^-2\pi^0$	**0.65/2.40/7.94**	
	Total	**18.9/28.3/34.1**	
$4\pi^0$	$[\kappa, \sigma \to \pi^0\pi^0]$	2.26/2.95/5.09	$g_{\sigma\kappa\bar{\kappa}}$, $g_{\sigma\pi^0\pi^0}$
	$[K^*, \sigma \to \pi^0\pi^0]$	5.89/16.9/35.9	$g_{\sigma\kappa\bar{K}^*}$, $g_{\sigma\pi^0\pi^0}$
	Total	**11.3/16.9/18.4**	

processes, the ratio of $\Gamma_{2\pi^+2\pi^-}/\Gamma_{\pi^+\pi^-2\pi^0}$ falls between these two limits. Comparing this ratio to experimental measurements can help clarify the decay mechanism of $f_0(1370)$, examining our scenario. Similarly, the ratio between the widths of the $4\pi^0$ state and the other 4π states can be used to estimate the contributions from the $\rho\rho$ intermediate state, as only the $\sigma\sigma$ intermediate state can contribute to the $4\pi^0$ final state.

The decay pattern for a broad state is not as accurate to define at a fixed energy as the narrow state, owing to its wide span mass distribution. The partial widths of some channels might be sensitive to the center-of-mass energy $\sqrt{s}$ over its distribution where some relevant thresholds are located. Hence, the well-defined branching ratios of different decay channels for a broad state, are generally obtained by integrating over its mass distribution, a process typically done in the experimental analysis. For a further reliable study on the decay pattern of the $f_0(1370)$, we present the dependence of the partial widths of different channels on the center-of-mass energy $\sqrt{s}$. We plot the partial widths of different channels varying along with the energy $\sqrt{s}$ with fixed coupling $g_{F\kappa\bar{\kappa}} = 35$ GeV and cutoff parameter $\alpha(\alpha_B) = 2(1)$ in Fig. 3.

As we can see from Figs. 3(a) and 3(b), with the increase of $\sqrt{s}$ from 1.1 to 1.7 GeV, the decay widths of the two-body channels such as $K\bar{K}$, $\pi\pi$, and $\eta\eta$ are stable, while for the four-body decay channels 4π and $K\bar{K}\pi\pi$, the decay width continuously increases along with the increase of $\sqrt{s}$. The dramatic increase in width of the $K\bar{K}\pi\pi$ channel is more evident in Fig. 3(b) than in Fig. 3(a) due to the scales. This phenomenon can be attributed to the increased phase space for the four-body decay and the threshold open for the $\kappa\bar{\kappa}$ and $\rho\rho$ intermediate states as $\sqrt{s}$ increases. The $\rho\rho$ threshold open effect is apparent as shown in Fig. 4, which will be discussed later. As a consequence of these threshold effects, the apparent line shape of the resonance varies depending on the specific decay channel, consistent with the analysis presented in [61]. From another perspective, the analytic continuation of a system with pole deep inside the complex plane can be highly nontrivial, and the projection onto the real axis, where experiments are performed, can differ widely depending on the complexity of the system. In Fig. 3 we can see that before energy point about 1.45 GeV, the largest contribution to the total width is from the $K\bar{K}$ channel, the order of these partial widths is $\Gamma_{K\bar{K}} > \Gamma_{4\pi} > \Gamma_{\pi\pi} > \Gamma_{\eta\eta} > \Gamma_{K\bar{K}\pi\pi}$. When $\sqrt{s}$ is larger than 1.45 GeV, the partial width of the 4π channel exceeds that of the $K\bar{K}$ channel, becoming the most dominant contribution. However, when $\sqrt{s}$ is less than about 1.34 GeV, the partial width of the 4π channel is even smaller than that of the $\pi\pi$ channel. Similarly, along with the increase of $\sqrt{s}$, the large difference between the partial widths of the $K\bar{K}\pi\pi$ and $\pi\pi$ channels at small $\sqrt{s}$ starts to reduce gradually.

Analysis on the $2\pi^+2\pi^-$ spectrum in [21] gives the ratio of $\mathrm{Br}(\rho^0\rho^0 \to 2\pi^+2\pi^-) : \mathrm{Br}(\sigma\sigma \to 2\pi^+2\pi^-)$ as 3:7. Our corresponding result shown in Table IV yields a much smaller $\rho\rho$ fraction, with $\rho^0\rho^0 : \sigma\sigma \approx 1:38$ and $\approx 1:12$ for the cutoff choices $\alpha(\alpha_B) = 2(1)$ and 3(2), respectively. Our calculations indicate that the strong suppression of the $\rho\rho$ channel relative to $\sigma\sigma$ is a distinct feature of the $\kappa\bar{\kappa}$ molecular picture. We note that our result is obtained at fixed energy $\sqrt{s} = 1.37$ GeV, while the experimental branching ratios are obtained by integrating over the mass distribution of $f_0(1370)$. The ratio is also sensitive to the parametrization of the σ, which we adopted differently from [21].

For a more reliable comparison, we plot the respective partial widths of these two parts varying along with the center-of-mass energy $\sqrt{s}$ in Fig. 4, to investigate the resulting trend of their ratio after performing the mass

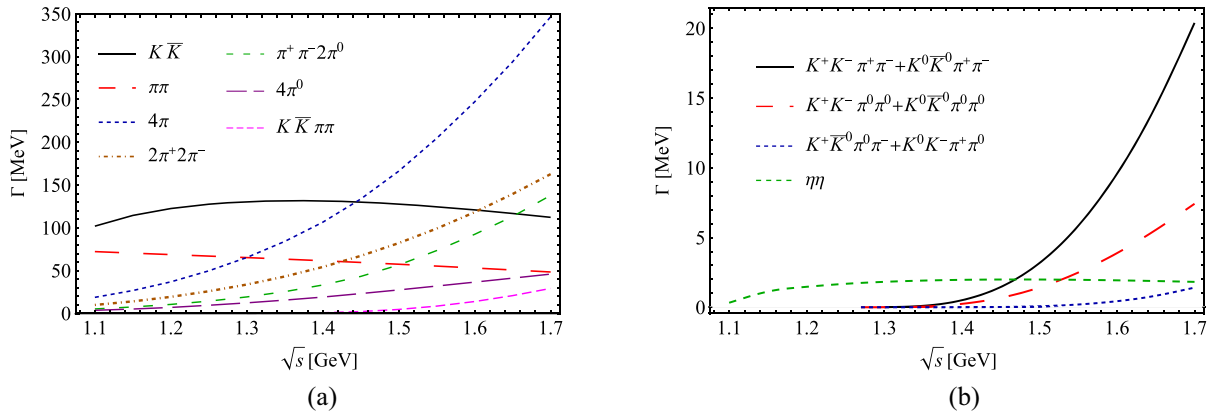


FIG. 3. Dependence of the partial widths of different channels on the center-of-mass energy $\sqrt{s}$ with fixed coupling $g_{F\kappa\bar{\kappa}} = 35$ GeV and cutoff parameter $\alpha(\alpha_B) = 2(1)$. Because the scales in widths for some channels are much smaller than others, we present them in two separate figures with distinct scale for clarity. (a) $K\bar{K}$, $\pi\pi$, 4π, and $K\bar{K}\pi\pi$ channels. Different specific 4π states are also presented. (b) $K\bar{K}\pi\pi$ and $\eta\eta$ channels. Different specific $K\bar{K}\pi\pi$ states are also presented. Note that $\Gamma(K^+K^-\pi^+\pi^-) = \Gamma(K^0\bar{K}^0\pi^+\pi^-)$, $\Gamma(K^+\bar{K}^0\pi^0\pi^-) = \Gamma(K^0K^-\pi^+\pi^0)$ and $\Gamma(K^+K^-\pi^0\pi^0) = \Gamma(K^0\bar{K}^0\pi^0\pi^0)$. For the $\eta\eta$ channel, $\Gamma(F \to \eta\eta)$ is presented.

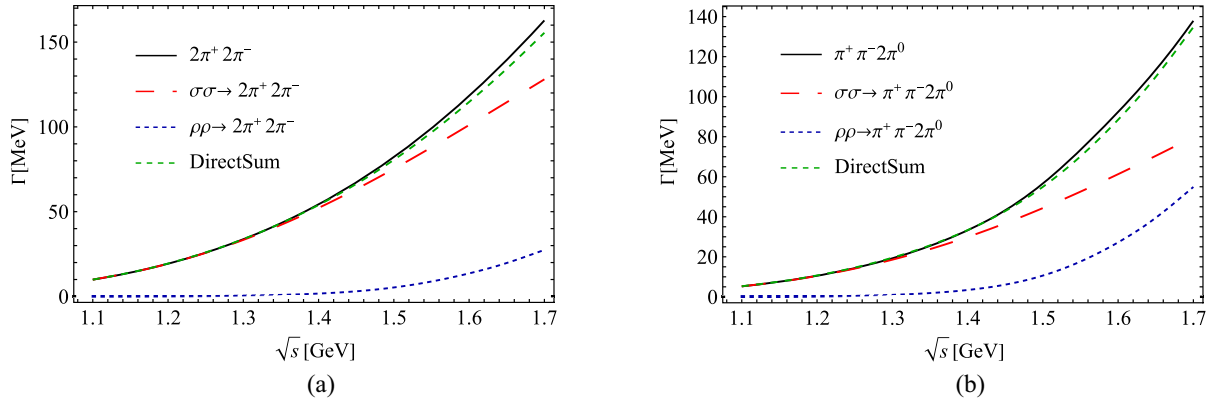


FIG. 4. Dependence of the partial widths of 4π states on the center-of-mass energy $\sqrt{s}$. Contributions from different intermediate channels $\sigma\sigma$ and $\rho\rho$ are also plotted. (a) For the $2\pi^+2\pi^-$ states. (b) For the $\pi^+\pi^-2\pi^0$ states.

distribution integration. Figures 4(a) and 4(b) refer to the $2\pi^+2\pi^-$ and $\pi^+\pi^-2\pi^0$ states, respectively. The black solid line indicates the total width of the specific 4π state, which includes the interference between the $\rho\rho$ and $\sigma\sigma$ intermediate states. The red long dashed line and the blue short dashed line indicate the exclusive widths from the $\sigma\sigma$ and $\rho\rho$ intermediate states, respectively. In Fig. 4(a), we observe that the increase in the $\sigma\sigma \to 4\pi$ process is moderate, whereas the $\rho\rho \to 4\pi$ process experiences a rapid increase once the energy $\sqrt{s}$ surpasses the $\rho\rho$ threshold. Nevertheless, even after considering the integration over the whole mass distribution, the $\rho\rho$ contribution remains insufficient compared to the ratios from experiments. The $\rho\rho$ contributions observed in experiments in $f_0(1370)$ decay to 4π may largely originate from the nearby $f_0(1500)$, which is suggested to be a $\rho\rho$ molecular state [18] and is expected to decay dominantly via the $\rho\rho$ channel. If the experimental analyses, typically relying on sums of Breit-Wigner functions, do not adequately separate these two broad overlapping resonances, the $\rho\rho$ events from $f_0(1500)$ decay would be misattributed to $f_0(1370)$, leading to an overestimation of the $\rho\rho$ branching fraction of $f_0(1370)$.

We also plot the direct sum of the exclusive widths of the $\rho\rho$ and $\sigma\sigma$ cases, which is indicated by a green dashed line and marked as "DirectSum" in Fig. 4. We find that it almost coincides with the black solid line along all the $\sqrt{s}$ for both the $2\pi^+2\pi^-$ and $\pi^+\pi^-2\pi^0$ channels, which implies that the $\rho\rho$ and $\sigma\sigma$ channels are almost orthogonal and their interference is negligible. This is because the $\rho\pi\pi$ vertex is of the P wave while the $\sigma\pi\pi$ vertex is of the S wave. Such a phenomenon is also confirmed in the analysis in Ref. [68].

In Table V, we collect the current available data and our theoretical results of the ratios between different decay channels as well as the ratios of the partial widths to the total width, which are calculated at fixed energy $\sqrt{s} = 1.37$ GeV. Again one should be cautious with the fact that some ratios are obtained by integrating over the mass distribution of $f_0(1370)$.

TABLE V. Collection of the available experiments and our results in the case of $\alpha(\alpha_B) = 1(0.5)/\mathbf{2}(\mathbf{1})/3(2)$. The coupling $g_{F\kappa\bar{\kappa}}$ is fixed to be 35 GeV. Boldface values correspond to the reference cutoff choice $\alpha(\alpha_B) = 2(1)$.

Expression	Experiment	Theory (fixed $\sqrt{s} = 1.37$ GeV)
$\Gamma(F \to K\bar{K})/\Gamma_F$	0.35 ± 0.13 [69]	$0.35/\mathbf{0.45}/0.49$
$\Gamma(F \to \pi\pi)/\Gamma_F$	0.26 ± 0.09 [69]; <0.10 [30]	$0.16/\mathbf{0.22}/0.25$
$\Gamma(F \to 4\pi)/\Gamma_F$	>0.72 [21]	$0.46/\mathbf{0.32}/0.25$
$\Gamma(F \to K\bar{K}\pi\pi)/\Gamma_F$	...	$2.5 \times 10^{-3}/\mathbf{1.1 \times 10^{-3}}/7.9 \times 10^{-4}$
$\Gamma(F \to K\bar{K})/\Gamma(F \to \pi\pi)$	0.08 ± 0.08 [52]; 0.46 ± 0.19 [41]; 0.91 ± 0.2 [70];	$2.15/\mathbf{2.10}/2.01$
$\Gamma(F \to \eta\eta)/\Gamma(F \to 4\pi)$	$(4.7 \pm 2.0) \times 10^{-3}$ [44]; $(28 \pm 11) \times 10^{-3}$ [71]	$11.7 \times 10^{-3}/\mathbf{21.0 \times 10^{-3}}/29.3 \times 10^{-3}$
$\Gamma'(F \to \eta\eta)/\Gamma(F \to 4\pi)$	$(4.7 \pm 2.0) \times 10^{-3}$ [44]; $(28 \pm 11) \times 10^{-3}$ [71]	$5.4 \times 10^{-4}/\mathbf{9.7 \times 10^{-4}}/1.3 \times 10^{-3}$
$\Gamma(F \to 4\pi)/\Gamma(F \to \pi\pi)$	0.3 ± 0.12 [53]; 0.1–0.25 [34]	$2.79/\mathbf{1.48}/1.02$
$\Gamma(F \to \rho\rho)/\Gamma(F \to 4\pi)$	0.26 ± 0.07 [24]	$0.02/\mathbf{0.04}/0.11$
$\Gamma(F \to \sigma\sigma)/\Gamma(F \to 4\pi)$	0.51 ± 0.09 [24]	$0.79/\mathbf{0.78}/0.74$
$\Gamma(F \to 2\pi^+2\pi^-)/\Gamma(F \to 4\pi)$	0.42 ± 0.014 [21]	$0.51/\mathbf{0.51}/0.50$
$\Gamma(F \to \pi^+\pi^-2\pi^0)/\Gamma(F \to 4\pi)$	0.512 ± 0.019 [21]	$0.31/\mathbf{0.31}/0.33$
$\Gamma(F \to \sigma\sigma \to 4\pi^0)/\Gamma(F \to 4\pi)$	0.068 ± 0.005 [21]; 0.27 ± 0.06 [24]	$0.18/\mathbf{0.18}/0.18$

From Table V we can see that for those decay channels "seen" in $f_0(1370)$ decay, no single experimental number on branching ratios nor ratios thereof has been determined because of conflicting results. This is quite different from the nearby $f_0(1500)$ with five well established branching ratios. As stated in [39], generally $f_0(1370)$ analyses suffer from some aspects of the "model problem": parametrization choices, most frequently Breit–Wigner (BW), K matrices, nonresonant backgrounds and isobars, *a priori* selection of decay channels, two body or quasi-two-body approximations, etc. Hence, most of the current data are model dependent. Indeed, the shape of such resonances changes with the dynamics of the process where they appear, therefore they must be rigorously identified from the process-independent associated poles.

In Table V, the relation between the $K\bar{K}$ and $\pi\pi$ channels has two kinds of results. Qualitatively, measurements from the $\pi\pi$ and πp scattering obtained at the mass of $f_0(1370)$ [69] support that $\Gamma(F \to K\bar{K})$ is larger than $\Gamma(F \to \pi\pi)$, which is consistent with our results at $\sqrt{s} = 1.37$ GeV. In contrast, measurements from the J/ψ hadronic decay [52], J/ψ radiative decay [48], the pp central production [41], and the $p\bar{p}$ annihilation at rest [70] show an inverse branching fraction ratio. As mentioned in the Introduction, the data of J/ψ hadronic decay recoiling against ϕ even gives a very small value for this ratio of 0.08 ± 0.08 due to the conspicuous signal in $\pi\pi$ but absence of any corresponding peak in K^+K^-. We attempt to explain this by the destructive interference between the two parts in the $f_0(1370)$ wave function: $s\bar{s}$ and the molecular component $\kappa\bar{\kappa}$. Although the $s\bar{s}$ component is not included in the wave function of Eq. (3) in our calculation above, a pure molecular state is unlikely to exist in reality, and the $f_0(1370)$ wave function could include a small $s\bar{s}$ component. $s\bar{s}$ is produced in J/ψ decay recoiling against ϕ as leading order and it strongly couples to $K\bar{K}$ but contributes to $\pi\pi$ with significantly weaker strength, leading to a possible destructive effect in the $K\bar{K}$ channel but not affecting the $\pi\pi$ channel. Such an $s\bar{s}$ destructive effect might also appear in the pp central production and J/ψ radiative decay but appear in the πp scattering with a smaller fraction. The more quantitative discussion about this issue is complex and needs more reliable analyses on experiments.

With the coupling $g_{\kappa K\eta}$, the theoretical ratio of the widths between $\eta\eta$ and 4π channels is consistent with the data in Ref. [71], while with the coupling $g'_{\kappa K\eta}$, this ratio is more consistent with the data in Ref. [44]. Whether the 4π channel is the most dominant one is also conflicting from the experimental ratios in Table V. The accurate analyses on the 4π spectra are difficult because it is hard to disentangle the contribution from $f_0(1370)$ and $f_0(1500)$ due to the subtle parametrization of the broad $f_0(1370)$. In most earlier work, the $f_0(1370)$ has been fitted with a Breit-Wigner amplitude of constant width. This is inaccurate because the resonance couples to 4π channel, which give rise to a strongly s-dependent width due to the rapid opening of the 4π thresholds for $\sigma\sigma$ and $\rho\rho$. As Achasov and Shestakov have emphasized [72], if one describes these spectra by an f_0 state with an energy-dependent total width its mass has to lie above 1500 MeV, and even no appreciable coupling of $f_0(1370)$ to the 4π channel is required. While we should still remain skeptical about this conclusion because it is also drawn based on the Breit-Wigner–like parametrization.

The analysis in Ref. [73] carefully considered the Bose symmetry interference effects and found that these effects cause the ratios between different specific 4π states to obviously differ from the naïve counting values without considering these effects, as what is evaluated in [21] based on the $\mathrm{Br}(2\pi^+2\pi^-)$ to obtain these ratios. Hence, the estimated ratios of $\mathrm{Br}(2\pi^+2\pi^-):\mathrm{Br}(\pi^+\pi^-2\pi^0):\mathrm{Br}(4\pi^0)$ in [21] are not reliable. Meanwhile such effects have been fully considered in our calculations.

IV. SUMMARY

In summary, motivated by the fact that the $f_0(980)$ and $f_0(1790)$ are, respectively, plausible $K\bar{K}$ and $K^*\bar{K}^*$ molecules and the phenomenology that the $f_0(980)$, $f_0(1370)$ and $f_0(1790)$ appear successively in the $\pi\pi$ spectrum in J/ψ hadronic decay recoiling against ϕ, where the $s\bar{s}$ is produced in leading order, we assume that $f_0(1370)$ is a $\kappa\bar{\kappa}$ molecular state and calculate the partial widths of various channels in $f_0(1370)$ decay, including $K\bar{K}$, $\pi\pi$, $\eta\eta$, 4π, and $K\bar{K}\pi\pi$. We treat the coupling $g_{F\kappa\bar{\kappa}}$ [F indicates $f_0(1370)$] as a free parameter and fit it to the measured total width of $f_0(1370)$ listed in the RPP, finding that this coupling should be in the range of 25–40 GeV with cutoff parameter $\alpha(\alpha_B) = 2(1) \sim 3(2)$. The decay pattern is independent of this coupling because it is a common coupling for all the decay channels.

At the nominal mass of $f_0(1370)$: $m_F = 1.37$ GeV and with $g_{F\kappa\bar{\kappa}} = 35$ GeV and $\alpha(\alpha_B) = 2(1)$, the $K\bar{K}$ channel has the largest partial width, followed by the 4π and $\pi\pi$ channels. The $\pi\pi$ and 4π channels have comparable partial widths. These three channels are the most dominant decay channels in $f_0(1370)$ decay. Different strategies for determining $\kappa K\eta$ coupling result in significant variations in the partial width of the $\eta\eta$ channel. We have found the distinct decay properties in $\eta\eta$ channel between $\kappa\bar{\kappa}$ and $K^*\overline{K^*}$ molecules, which can be examined in the BESIII data of $J/\psi \to \phi\eta\eta$. The partial width of the $K\bar{K}\pi\pi$ channel is about 300 keV in total. Notice that although the $K\bar{K}\pi\pi$ channel proceeds through tree-level decay, it has very limited four-body phase space around 1.37 GeV.

We also test the dependence of the partial widths of different channels on the center-of-mass energy $\sqrt{s}$. The decay widths of the two-body channels such as $K\bar{K}$, $\pi\pi$, and $\eta\eta$ are stable with the variation of $\sqrt{s}$, while the decay

widths of the four-body decay channels 4π and $K\bar{K}\pi\pi$ continuously increase along with the increase of $\sqrt{s}$. With $\sqrt{s}$ larger than 1.45 GeV, the partial width of the 4π channel exceeds that of the $K\bar{K}$ channel, becoming the most dominant decay channel. Such phenomenon might cause different manifestation of $f_0(1370)$ in different spectra.

Not all of the ratios reflecting the decay pattern in our calculations are consistent with the current data, such as the 4π dominant conclusion and the ratio of $K\bar{K}$ over $\pi\pi$ in some measurements. However, in $f_0(1370)$ decay, most of the current data are model dependent, relying on fitting sums of Breit-Wigner functions and no single experimental number on branching ratios or ratios thereof are determined because they are conflicting. Hence, these inconsistencies cannot rule out the $\kappa\bar{\kappa}$ assignment for $f_0(1370)$. The small $K\bar{K}$ branching ratio due to the absence of a corresponding peak in $K\bar{K}$ spectrum, such as in J/ψ hadronic decay recoiling against ϕ, contradicts with our result. We attempt to explain that by the destructive interference in decay to $K\bar{K}$ between the $s\bar{s}$ and $\kappa\bar{\kappa}$ components in the $f_0(1370)$ wave function. The 4π spectra are also elusive because it is hard to disentangle the contribution from $f_0(1370)$ and $f_0(1500)$ due to the strongly s-dependent width of $f_0(1370)$. The ratios between different 4π states can be related to decay mechanisms as the intermediate states $\rho\rho$ and $\sigma\sigma$ have distinct features in 4π decay. In our $\kappa\bar{\kappa}$ molecular picture, the $\sigma\sigma$ channel dominates over $\rho\rho$, which is inconsistent with current data. The $\rho\rho$ signal observed in the $f_0(1370)$ region may largely originate from the nearby $f_0(1500)$, a $\rho\rho$ molecular candidate whose $\rho\rho \to 4\pi$ events can be misattributed to $f_0(1370)$ in experimental analyses that do not adequately separate these two broad overlapping resonances.

This work relies on a number of model assumptions that should be kept in mind when interpreting the results: (i) the pure $\kappa\bar{\kappa}$ molecular ansatz of Eq. (3) without $s\bar{s}$ or other mixing components. (ii) the simple-pole propagators $1/(s - s_{\rm pole})$ for the broad intermediate states κ and σ. (iii) the approximate SU(3) flavor symmetry relations applied to the lowest scalars. (iv) the reliance on particular phenomenological determinations of couplings from the literature, which carry their own model dependence and uncertainties. (v) the coupling estimation methods such as the spectator approximation used to estimate the couplings involving κ and σ. (vi) the specific choice of the monopole form factor and the cutoff parameter for the exchanged states. Despite these limitations, the model provides useful qualitative insights into the decay pattern expected for a $\kappa\bar{\kappa}$ molecular interpretation of $f_0(1370)$.

We need further reliable analyses on the $f_0(1370)$ in both theoretical and experimental aspects. The BESIII Collaboration has recorded data with significantly improved quality and statistics. They can attempt to search for the $f_0(1370)$ signal in the $K\bar{K}\pi\pi/4\pi/\eta\eta$ channels in J/ψ hadronic decays recoiling against ϕ. Such measurements can help us to test the $\kappa\bar{\kappa}$ molecule assignment for $f_0(1370)$. The pattern for the different specific $K\bar{K}\pi\pi/4\pi$ states also has a unique feature in this scenario, which can be used as a further check.

ACKNOWLEDGMENTS

The authors appreciate the useful discussions with Feng-Kun Guo, Jia-Jun Wu, Xiong-Hui Cao, Shu-Ming Wu, Zhen-Hua Zhang, Zhao-Sai Jia, and Xu Zhang.

DATA AVAILABILITY

There are no publicly available research data or software supporting this manuscript. Requests for further information or data should be sent to the authors.

APPENDIX A: ISOSPIN CONVENTIONS

Let I be an isospin operator in the Hilbert space, and its corresponding isospin transform matrix is $\boldsymbol{\tau}/2$. As discussed in Ref. [74], due to the fact that $\hat{C}$ does not commute with the step operators $I_1 \pm iI_2$, the relative phases of the antiparticle states will not satisfy the following requirement

$$(I_1 \pm iI_2)|\mathrm{Im}\rangle = +\sqrt{(I \mp m)(I \pm m + 1)}|I, m \pm 1\rangle. \quad \text{(A1)}$$

Both of the deficiencies are removed by constructing the antiparticle isospin multiplet, which is denoted by $\overline{|\mathrm{Im}\rangle}$, with the help of the G-conjugation operator,

$$\begin{aligned}\overline{|\mathrm{Im}\rangle} &\equiv \eta_I \hat{G}|\mathrm{Im}\rangle, \\ &= \eta_I(-1)^{I-m}\hat{C}|I, -m\rangle. \end{aligned} \quad \text{(A2)}$$

η_I is chosen to be -1 as discussed in [74].

We take the convention as $\kappa^+ = |1/2, 1/2\rangle$, $\kappa^0 = |1/2, -1/2\rangle$, and we construct the isospin states of antiparticles using the prescription given by Eq. (A2). It is a natural choice to take positive charge parity for κ particles as the neutral scalars 0^{++},

$$\hat{C}|\kappa^+\rangle = +|\kappa^-\rangle, \qquad \hat{C}|\kappa^0\rangle = +|\bar{\kappa}^0\rangle, \quad \text{(A3)}$$

$$\begin{aligned}|1/2, -1/2\rangle &= (-1) \times (-1)^{1/2-(-1/2)}\hat{C}|1/2, 1/2\rangle \\ &= \hat{C}|\kappa^+\rangle \\ &= +|\kappa^-\rangle \end{aligned} \quad \text{(A4)}$$

$$|1/2, 1/2\rangle = (-1) \times (-1)^{1/2-(1/2)}\hat{C}|1/2, -1/2\rangle \quad \text{(A5)}$$

$$= -\hat{C}|\kappa^0\rangle \quad \text{(A6)}$$

$$= -|\bar{\kappa}^0\rangle \quad \text{(A7)}$$

TABLE VI. Conventions for isospin states and flavor wave functions of the particles involved in this work.

Particles	Isospin state	Flavor wave function
π^+	$-\|1,1\rangle$	$u\bar{d}$
π^0	$\|1,0\rangle$	$(1/\sqrt{2})(u\bar{u}-d\bar{d})$
π^-	$\|1,-1\rangle$	$d\bar{u}$
κ^+/K^+	$\|1/2,1/2\rangle$	$u\bar{s}$
κ^0/K^0	$\|1/2,-1/2\rangle$	$d\bar{s}$
$\bar{\kappa}^0/\bar{K}^0$	$-\|1/2,1/2\rangle$	$s\bar{d}$
κ^-/K^-	$\|1/2,-1/2\rangle$	$s\bar{u}$

Hence, the antiparticle isospin states are $\bar{\kappa}^0=-|1/2,1/2\rangle$, $\kappa^-=|1/2,-1/2\rangle$. The adopted convention in our work of the isospin states of the particles is shown in Table VI.

APPENDIX B: ESTIMATIONS OF THE EFFECTIVE COUPLING CONSTANTS

1. $\rho\kappa\bar{\kappa}$

We assume κ to be a molecular state consisting of $K\pi$, its couplings to other states can be described as follows: the $\kappa\to V\kappa/S\kappa$ interaction can be viewed as one of the pseudoscalar components inside κ interacting with the vector or scalar, while the other component acts approximately as a spectator. For example, the $\kappa\kappa\rho$ vertex can be approximately related to the $\rho\pi\pi$ and $\rho K\bar{K}$ couplings by guaranteeing that the $K\pi$ is projected to the isospin state of κ. In the molecular picture, the flavor wave function of κ can be expressed as

$$\kappa^+=\frac{1}{\sqrt{3}}|K^+\pi^0\rangle+\frac{\sqrt{2}}{\sqrt{3}}|K^0\pi^+\rangle, \tag{B1}$$

$$\kappa^0=\frac{\sqrt{2}}{\sqrt{3}}|K^+\pi^-\rangle-\frac{1}{\sqrt{3}}|K^0\pi^0\rangle. \tag{B2}$$

Based on the $g_{K^{*0}K^+\pi^-}$ we can obtain the $g_{\rho K\bar{K}}$ and $g_{\omega K\bar{K}}$ couplings by the SU(3) flavor symmetry. By the Lagrangian with SU(3) symmetry, the vertex coupling constants are connected as follows [59]:

$$g_{VPP}=g_{K^{*0}K^+\pi^-}, \tag{B3}$$

$$g_{\rho K^+K^-}=-g_{VPP}/\sqrt{2}, \tag{B4}$$

$$g_{\rho^0\pi^+\pi^-}=-\sqrt{2}g_{VPP}. \tag{B5}$$

The possible interactions between ρ and the pseudoscalar components inside κ^+ will include $\rho^0K^+K^-$, $\rho^0K^0\bar{K}^0$, and $\rho^0\pi^+\pi^-$. The coupling $\rho^0\kappa^+\kappa^-$ can be calculated as

$$\begin{aligned}g_{\rho^0\kappa^+\kappa^-}&=\frac{1}{3}g_{\rho^0K^+K^-}+\frac{2}{3}(g_{\rho^0K^0\bar{K}^0}+g_{\rho^0\pi^+\pi^-})\\&=\frac{1}{3}\left(\frac{-g_{VPP}}{\sqrt{2}}\right)+\frac{2}{3}\left(\frac{g_{VPP}}{\sqrt{2}}-\sqrt{2}g_{VPP}\right)\\&=\frac{-g_{VPP}}{\sqrt{2}}\\&=g_{\rho^0K^+K^-}.\end{aligned} \tag{B6}$$

The decomposition of the vertex $\rho^+\kappa^+\bar{\kappa}^0$ is

$$\begin{aligned}g_{\rho^+\kappa^+\bar{\kappa}^0}=&\frac{\sqrt{2}}{\sqrt{3}}\times\frac{-1}{\sqrt{3}}g_{\rho^+\pi^+\pi^0}+\frac{1}{\sqrt{3}}\\&\times\frac{-1}{\sqrt{3}}g_{\rho^+K^+\bar{K}^0}+\frac{1}{\sqrt{3}}\times\frac{\sqrt{2}}{\sqrt{3}}g_{\rho^+\pi^0\pi^+},\end{aligned} \tag{B7}$$

with SU(3) symmetry, $g_{\rho^+K^+\bar{K}^0}=-g_{VPP}$, $g_{\rho^+\pi^+\pi^0}=\sqrt{2}g_{VPP}$, and $g_{\rho^+\pi^0\pi^+}=-\sqrt{2}g_{VPP}$, we have

$$g_{\rho^+\kappa^+\bar{\kappa}^0}=-g_{VPP}=g_{\rho^+K^+\bar{K}^0}. \tag{B8}$$

Similarly, we have

$$\begin{aligned}g_{\rho^0\kappa^0\bar{\kappa}^0}&=\frac{1}{3}g_{\rho^0K^0\bar{K}^0}+\frac{2}{3}(g_{\rho^0K^+K^-}+g_{\rho^0\pi^-\pi^+})\\&=\frac{1}{3}\left(\frac{g_{VPP}}{\sqrt{2}}\right)+\frac{2}{3}\left(\frac{-g_{VPP}}{\sqrt{2}}+\sqrt{2}g_{VPP}\right)\\&=\frac{g_{VPP}}{\sqrt{2}}\\&=g_{\rho^0K^0\bar{K}^0}.\end{aligned} \tag{B9}$$

2. $\sigma\kappa\bar{\kappa}$

Regarding the σ as a $\pi\pi$ molecular state, its wave function can be written as

$$\sigma=\frac{-1}{\sqrt{3}}|\pi^0\pi^0\rangle+\frac{-1}{\sqrt{3}}|\pi^+\pi^-\rangle+\frac{-1}{\sqrt{3}}|\pi^-\pi^+\rangle. \tag{B10}$$

A similar decomposition for $g_{\sigma\kappa^+\kappa^-}$ coupling can be written as

$$\begin{aligned}g_{\sigma\kappa^+\kappa^-}&=\frac{1}{3}(2g_{\sigma\pi^0\pi^0})+\frac{1}{3}g_{\sigma K^+K^-}+\frac{2}{3}g_{\sigma\pi^+\pi^-}+\frac{2}{3}g_{\sigma K^0\bar{K}^0}\\&=3g_{\sigma K^+K^-},\end{aligned} \tag{B11}$$

$$\begin{aligned}g_{\sigma\kappa^0\bar{\kappa}^0}&=\frac{1}{3}(2g_{\sigma\pi^0\pi^0})+\frac{1}{3}g_{\sigma K^0\bar{K}^0}+\frac{2}{3}g_{\sigma\pi^+\pi^-}+\frac{2}{3}g_{\sigma K^+K^-}.\\&=3g_{\sigma K^0\bar{K}^0}.\end{aligned} \tag{B12}$$

The factor of 2 multiplying $g_{\sigma\pi^0\pi^0}$ accounts for the two distinct contractions of the identical π^0 fields.

3. $\sigma\kappa\bar{K}^*$

Similarly, one of the components inside the σ is assumed to act as a spectator in the interaction, then the coupling of $\sigma\kappa\bar{K}^*$ vertex can be approximately related to the coupling of $K^*K\pi$ vertex. For example, based on the wave functions of σ and κ, the coupling $g_{\sigma\kappa^+K^{*-}}$ can be expressed as

$$\begin{aligned} g_{\sigma\kappa^+K^{*-}} &= \frac{-1}{\sqrt{3}}\times\frac{1}{\sqrt{3}}\cdot g_{K^{*-}K^-\pi^0} - \frac{1}{\sqrt{3}}\times\frac{\sqrt{2}}{\sqrt{3}}\cdot g_{K^{*-}\bar{K}^0\pi^-} \\ &= \frac{-1}{3}\times\left(\frac{-g_{VPP}}{\sqrt{2}}\right) - \frac{\sqrt{2}}{3}(-g_{VPP}) \\ &= \frac{g_{VPP}}{\sqrt{2}}, \end{aligned} \tag{B13}$$

and the $g_{\sigma\kappa^0\bar{K}^{*0}}$ can be expressed as

$$\begin{aligned} g_{\sigma\kappa^0\bar{K}^{*0}} &= \frac{-1}{\sqrt{3}}\times\frac{-1}{\sqrt{3}}\cdot g_{\bar{K}^{*0}\bar{K}^0\pi^0} - \frac{1}{\sqrt{3}}\times\frac{\sqrt{2}}{\sqrt{3}}\cdot g_{\bar{K}^{*0}K^-\pi^+} \\ &= \frac{1}{3}\cdot\frac{g_{VPP}}{\sqrt{2}} - \frac{\sqrt{2}}{3}\cdot(-g_{VPP}) \\ &= \frac{g_{VPP}}{\sqrt{2}}. \end{aligned} \tag{B14}$$

4. $\rho\kappa\bar{K}^*$

Assuming $g_{\sigma\pi\pi} = g_{\sigma\rho\rho}$ due to the identical flavor wave functions for π and ρ and based on the flavor SU(3) symmetry, we have $g_{\sigma\rho^+\rho^-} = \sqrt{2}g_{VVS} = -0.79 + 2.84i$ GeV and $g_{\rho^0\kappa^+K^{*-}} = g_{VVS}/\sqrt{2} = -0.39 + 1.42i$.

APPENDIX C: ISSUES ABOUT THE η-η' MIXING

If the η state is treated as a pure octet η_8 as in Ref. [66], the octet matrix

$$P_8 = \begin{pmatrix} \frac{1}{\sqrt{2}}\pi^0 + \frac{1}{\sqrt{6}}\eta_8 & \pi^+ & K^+ \\ \pi^- & -\frac{1}{\sqrt{2}}\pi^0 + \frac{1}{\sqrt{6}}\eta_8 & K^0 \\ K^- & \bar{K}^0 & -\frac{2}{\sqrt{6}}\eta_8 \end{pmatrix} \tag{C1}$$

is used.

However, the SU(3) flavor symmetry is slightly broken, which leads to the mixing of the singlet η_1 and the octet η_8. Hence, the physical states η and η' are the outcomes of the mixing of η_1 and η_8. Defining a mixing angle θ in the $\eta_8 - \eta_1$ basis, the mixing scheme is

$$\begin{pmatrix} \eta \\ \eta' \end{pmatrix} = \begin{pmatrix} \cos\theta & -\sin\theta \\ \sin\theta & \cos\theta \end{pmatrix}\begin{pmatrix} \eta_8 \\ \eta_1 \end{pmatrix}, \tag{C2}$$

and

$$\begin{pmatrix} \eta_8 \\ \eta_1 \end{pmatrix} = \begin{pmatrix} \cos\theta & \sin\theta \\ -\sin\theta & \cos\theta \end{pmatrix}\begin{pmatrix} \eta \\ \eta' \end{pmatrix}. \tag{C3}$$

Incorporating the mixing, a U(3) flavor symmetry matrix, which is the sum of the octet and singlet matrices, can be adopted as shown in [75], i.e.,

$$\begin{aligned} U &= P + \frac{\eta_1}{\sqrt{3}}\mathbb{1}_{3\times3} \\ &= \begin{pmatrix} \frac{1}{\sqrt{2}}\pi^0 + \frac{1}{\sqrt{6}}\eta_8 + \frac{1}{\sqrt{3}}\eta_1 & \pi^+ & K^+ \\ \pi^- & -\frac{1}{\sqrt{2}}\pi^0 + \frac{1}{\sqrt{6}}\eta_8 + \frac{1}{\sqrt{3}}\eta_1 & K^0 \\ K^- & \overline{K^0} & -\frac{2}{\sqrt{6}}\eta_8 + \frac{1}{\sqrt{3}}\eta_1 \end{pmatrix}. \end{aligned} \tag{C4}$$

For determining the coupling of η, we can replace the η_8 and η_1 in terms of η and η' based on Eq. (C3).

Expanding the effective Lagrangian $\mathcal{L} = g_{SPP}\langle SPP\rangle$ with the pseudoscalar matrix U under the U(3) flavor symmetry, we have

$$\mathcal{L}_{\kappa K\eta} = g_{SPP}\left[\left(\frac{1}{\sqrt{6}} - \frac{2}{\sqrt{6}}\right)\kappa K\eta_8 + \frac{2}{\sqrt{3}}\kappa K\eta_1\right] = g_{SPP}\left[\frac{-1}{\sqrt{6}}\cos\theta + \frac{2}{\sqrt{3}}(-\sin\theta)\right]\kappa K\eta \tag{C5}$$

and

$$\mathcal{L}_{\kappa K\pi^+} = g_{SPP}\kappa K\pi^+. \tag{C6}$$

In our work, we adopt $\theta \approx -10.7°$. As shown in Table I, this yields a coupling ratio $|g_{\kappa K\pi^\pm}|/|g'_{\kappa K\eta}| \approx 5.4$.

[1] V. Baru, J. Haidenbauer, C. Hanhart, Y. Kalashnikova, and A. E. Kudryavtsev, Evidence that the $a_0(980)$ and $f_0(980)$ are not elementary particles, Phys. Lett. B **586**, 53 (2004).

[2] G. 't Hooft, G. Isidori, L. Maiani, A. D. Polosa, and V. Riquer, A theory of scalar mesons, Phys. Lett. B **662**, 424 (2008).

[3] J. A. Oller and E. Oset, Chiral symmetry amplitudes in the S wave isoscalar and isovector channels and the σ, $f_0(980)$, $a_0(980)$ scalar mesons, Nucl. Phys. **A620**, 438 (1997); **A652**, 407(E) (1999).

[4] R. L. Jaffe, Multiquark hadrons. I. Phenomenology of $Q^2\bar{Q}^2$ mesons, Phys. Rev. D **15**, 267 (1977).

[5] J. R. Pelaez, On the nature of light scalar mesons from their large-N_c behavior, Phys. Rev. Lett. **92**, 102001 (2004).

[6] T. Barnes, Two photon decays support the $(K\bar{K})$-molecule picture of the $S^*(975)$ and $\delta(980)$, Phys. Lett. **165B**, 434 (1985).

[7] F. E. Close, N. Isgur, and S. Kumano, Scalar mesons in ϕ radiative decay: Their implications for spectroscopy and for studies of CP violation at ϕ factories, Nucl. Phys. **B389**, 513 (1993).

[8] S. Navas *et al.* (Particle Data Group), Review of particle physics, Phys. Rev. D **110**, 030001 (2024).

[9] C. Amsler and F. E. Close, Is $f_0(1500)$ a scalar glueball?, Phys. Rev. D **53**, 295 (1996).

[10] C. Amsler and F. E. Close, Evidence for a scalar glueball, Phys. Lett. B **353**, 385 (1995).

[11] F. E. Close and Q. Zhao, Production of $f_0(1710)$, $f_0(1500)$, and $f_0(1370)$ in J/ψ hadronic decays, Phys. Rev. D **71**, 094022 (2005).

[12] F. Giacosa, T. Gutsche, V. E. Lyubovitskij, and A. Faessler, Scalar nonet quarkonia and the scalar glueball: Mixing and decays in an effective chiral approach, Phys. Rev. D **72**, 094006 (2005).

[13] P. Chatzis, A. Faessler, T. Gutsche, and V. E. Lyubovitskij, Hadronic and radiative three-body decays of J/ψ involving the scalars $f_0(1370)$, $f_0(1500)$ and $f_0(1710)$, Phys. Rev. D **84**, 034027 (2011).

[14] V. Vento, Glueball-meson mixing, Eur. Phys. J. A **52**, 1 (2016).

[15] R. Molina, D. Nicmorus, and E. Oset, The $\rho\rho$ interaction in the hidden gauge formalism and the $f_0(1370)$ and $f_2(1270)$ resonances, Phys. Rev. D **78**, 114018 (2008).

[16] D. Gülmez, U. G. Meißner, and J. A. Oller, A chiral covariant approach to $\rho\rho$ scattering, Eur. Phys. J. C **77**, 460 (2017).

[17] L. S. Geng and E. Oset, Vector meson-vector meson interaction in a hidden gauge unitary approach, Phys. Rev. D **79**, 074009 (2009).

[18] Z.-L. Wang and B.-S. Zou, $\rho\rho$ scattering revisited with coupled channels of pseudoscalar mesons, Phys. Rev. D **99**, 096014 (2019).

[19] L.-K. Yang, Z.-L. Wang, J.-J. Wu, and B.-S. Zou, Two-photon production of f_0 and a_0 resonances as hadronic molecules composed of two vector mesons, Phys. Rev. D **110**, 036020 (2024).

[20] A. Bettini, M. Cresti, S. Limentani, L. Bertanza, and A. Bigi, Evidence for a strong, possibly resonant, scalar $\rho\rho$ interaction, Nuovo Cimento A **42**, 695 (1966).

[21] M. Gaspero, Evidence for the dominance of an $I^GJ^{PC} = 0^+0^{++}$ resonance in $\bar{p}n \to 2\pi^+3\pi^-$ annihilation at rest, Nucl. Phys. **A562**, 407 (1993).

[22] C. Amsler *et al.* (Crystal Barrel Collaboration), Observation of a scalar resonance decaying to $\pi^+\pi^-\pi^0\pi^0$ in $\bar{p}p$ annihilation at rest, Phys. Lett. B **322**, 431 (1994).

[23] A. Abele *et al.* (Crystal Barrel Collaboration), Study of f_0 decays into four neutral pions, Eur. Phys. J. C **19**, 667 (2001).

[24] A. Abele *et al.* (Crystal Barrel Collaboration), 4π-decays of scalar and vector mesons, Eur. Phys. J. C **21**, 261 (2001).

[25] C. Amsler *et al.* (Crystal Barrel Collaboration), Proton-antiproton annihilation into $\eta\eta\pi$-Observation of a scalar resonance decaying into $\eta\eta$, Phys. Lett. B **291**, 347 (1992).

[26] V. V. Anisovich *et al.* (Crystal barrel Collaboration), Observation of two $J^{PC} = 0^{++}$ isoscalar resonances at 1365 and 1520 MeV, Phys. Lett. B **323**, 233 (1994).

[27] C. Amsler *et al.*, High statistics study of $f_0(1500)$ decay into $\pi^0\pi^0$, Phys. Lett. B **342**, 433 (1995).

[28] A. Abele *et al.*, Further analysis of $\bar{p}p \to 3\pi^0$, $\eta\eta\pi^0$ and $\eta\pi^0\pi^0$ at rest, Nucl. Phys. **A609**, 562 (1996); **A625**, 899(E) (1997).

[29] E. Klempt and A. Zaitsev, Glueballs, hybrids, multiquarks. Experimental facts versus QCD inspired concepts, Phys. Rep. **454**, 1 (2007).

[30] W. Ochs, The status of glueballs, J. Phys. G **40**, 043001 (2013).

[31] T. A. Armstrong *et al.* (E760 Collaboration), Evidence for $\eta\eta$ resonances in $\bar{p}p$ annihilations at $2950 < \sqrt{s} < 3620$-MeV, Phys. Lett. B **307**, 394 (1993).

[32] C. Amsler *et al.* (Crystal Barrel Collaboration), Proton Antiproton annihilation at 900- MeV/c into $\pi^0\pi^0\pi^0$, $\pi^0\pi^0\eta$ and $\pi^0\eta\eta$, Eur. Phys. J. C **23**, 29 (2002).

[33] I. Uman, D. Joffe, Z. Metreveli, K. K. Seth, A. Tomaradze, and P. K. Zweber, Light quark resonances in $p\bar{p}$ annihilations at 5.2- GeV/c, Phys. Rev. D **73**, 052009 (2006).

[34] D. V. Bugg, A study in depth of $f_0(1370)$, Eur. Phys. J. C **52**, 55 (2007).

[35] D. H. Cohen, D. S. Ayres, R. Diebold, S. L. Kramer, A. J. Pawlicki, and A. B. Wicklund, Amplitude analysis of the K^-K^+ system produced in the reactions $\pi^-p \to K^-K^+n$ and $\pi^+n \to K^-K^+p$ at 6- GeV/c, Phys. Rev. D **22**, 2595 (1980).

[36] V. A. Polychronakos, N. M. Cason, J. M. Bishop, N. N. Biswas, V. P. Kenney, D. S. Rhines, R. C. Ruchti, W. D. Shephard, M. J. Stangl, and J. M. Watson, Study of the reaction $\pi^-p \to nK_S^0K_S^0$ at 6.0-GeV/c and 7.0-GeV/c, Phys. Rev. D **19**, 1317 (1979).

[37] A. D. Martin and E. N. Ozmutlu, Analyses of $K\bar{K}$ production and scalar mesons, Nucl. Phys. **B158**, 520 (1979).

[38] A. Etkin *et al.*, Amplitude analysis of the $K_S^0K_S^0$ system produced in the reaction $\pi^-p \to K_S^0K_S^0n$ at 23-GeV/c, Phys. Rev. D **25**, 1786 (1982).

[39] J. R. Pelaez, A. Rodas, and J. R. de Elvira, $f_0(1370)$ controversy from dispersive meson-meson scattering data analyses, Phys. Rev. Lett. **130**, 051902 (2023); **132**, 239901(E) (2024).

[40] D. Barberis *et al.* (WA102 Collaboration), A partial wave analysis of the centrally produced $\pi^+\pi^-$ system in pp interactions at 450-GeV/c, Phys. Lett. B **453**, 316 (1999).

[41] D. Barberis *et al.* (WA102 Collaboration), A coupled channel analysis of the centrally produced K^+K^- and $\pi^+\pi^-$ final states in pp interactions at 450-GeV/c, Phys. Lett. B **462**, 462 (1999).
[42] D. Barberis *et al.* (WA102 Collaboration), A partial wave analysis of the centrally produced K^+K^- and $K^0_SK^0_S$ systems in pp interactions at 450-GeV/c and new information on the spin of the $f_J(1710)$, Phys. Lett. B **453**, 305 (1999).
[43] J. Adam *et al.* (STAR Collaboration), Measurement of the central exclusive production of charged particle pairs in proton-proton collisions at $\sqrt{s} = 200$ GeV with the STAR detector at RHIC, J. High Energy Phys. 07 (2020) 178.
[44] D. Barberis *et al.* (WA102 Collaboration), A Study of the $\eta\eta$ channel produced in central pp interactions at 450-GeV/c, Phys. Lett. B **479**, 59 (2000).
[45] S. Dobbs, A. Tomaradze, T. Xiao, and K. K. Seth, Comprehensive study of the radiative decays of J/ψ and $\psi(2S)$ to pseudoscalar meson pairs, and search for glueballs, Phys. Rev. D **91**, 052006 (2015).
[46] M. Ablikim *et al.* (BESIII Collaboration), Amplitude analysis of the $\pi^0\pi^0$ system produced in radiative J/ψ decays, Phys. Rev. D **92**, 052003 (2015); **93**, 039906(E) (2016).
[47] M. Ablikim *et al.* (BESIII Collaboration), Amplitude analysis of the K_SK_S system produced in radiative J/ψ decays, Phys. Rev. D **98**, 072003 (2018).
[48] A. V. Sarantsev, I. Denisenko, U. Thoma, and E. Klempt, Scalar isoscalar mesons and the scalar glueball from radiative J/ψ decays, Phys. Lett. B **816**, 136227 (2021).
[49] P. Minkowski and W. Ochs, B decays into light scalar particles and glueball, Eur. Phys. J. C **39**, 71 (2005).
[50] M. Ablikim *et al.* (BES Collaboration), Study of $J/\psi \to \omega K^+K^-$, Phys. Lett. B **603**, 138 (2004).
[51] M. Ablikim *et al.* (BES Collaboration), The σ pole in $J/\psi \to \omega\pi^+\pi^-$, Phys. Lett. B **598**, 149 (2004).
[52] M. Ablikim *et al.* (BES Collaboration), Resonances in $J/\psi \to \phi\pi^+\pi^-$ and ϕK^+K^-, Phys. Lett. B **607**, 243 (2005).
[53] M. Albaladejo and J. A. Oller, Identification of a scalar glueball, Phys. Rev. Lett. **101**, 252002 (2008).
[54] R. Aaij *et al.* (LHCb Collaboration), Study of the doubly charmed tetraquark T^+_{cc}, Nat. Commun. **13**, 3351 (2022).
[55] Y. Cheng, L. Qiu, and Q. Zhao, On the widths of $\eta(1295)$ and $\eta(1405/1475)$, arXiv:2302.01210.
[56] M. Hoferichter, J. R. de Elvira, B. Kubis, and U.-G. Meißner, Nucleon resonance parameters from Roy-Steiner equations, Phys. Lett. B **853**, 138698 (2024).
[57] R. Garcia-Martin, R. Kaminski, J. R. Pelaez, and J. Ruiz de Elvira, Precise determination of the $f_0(600)$ and $f_0(980)$ pole parameters from a dispersive data analysis, Phys. Rev. Lett. **107**, 072001 (2011).
[58] J. R. Peláez and A. Rodas, Dispersive $\pi K \to \pi K$ and $\pi\pi \to K\bar{K}$ amplitudes from scattering data, threshold parameters, and the lightest strange resonance κ or $K^*_0(700)$, Phys. Rep. **969**, 1 (2022).
[59] Y. Cheng and Q. Zhao, Hadronic loop effects on the radiative decays of the first radial excitations of η and η', Phys. Rev. D **105**, 076023 (2022).
[60] R. Kaminski, G. Mennessier, and S. Narison, Gluonium nature of the $\sigma/f_0(600)$ from its coupling to $K\bar{K}$, Phys. Lett. B **680**, 148 (2009).
[61] Y. Cheng, L. Qiu, and Q. Zhao, Understanding the non-trivial isoscalar pseudoscalar structures in the $K_SK_S\pi^0$ spectra in the J/ψ radiative decay, Phys. Rev. D **111**, 114015 (2025).
[62] H.-Y. Cheng, C.-K. Chua, and A. Soni, Final state interactions in hadronic B decays, Phys. Rev. D **71**, 014030 (2005).
[63] F.-K. Guo, C. Hanhart, G. Li, U.-G. Meissner, and Q. Zhao, Effect of charmed meson loops on charmonium transitions, Phys. Rev. D **83**, 034013 (2011).
[64] S. Weinberg, Elementary particle theory of composite particles, Phys. Rev. **130**, 776 (1963).
[65] S. Weinberg, Evidence that the deuteron is not an elementary particle, Phys. Rev. **137**, B672 (1965).
[66] Z.-L. Wang and B.-S. Zou, Further study of $f_0(1710)$ with the coupled-channel approach and the hadron molecular picture, Phys. Rev. D **104**, 114001 (2021).
[67] J. R. Peláez, A. Rodas, and J. Ruiz de Elvira, Strange resonance poles from $K\pi$ scattering below 1.8 GeV, Eur. Phys. J. C **77**, 91 (2017).
[68] A. V. Anisovich, D. V. Bugg, N. Djaoshvili, C. Hodd, J. Kisiel, L. Montanet, A. V. Sarantsev, and B. S. Zou, Resonances in $p\bar{p} \to \eta\pi^+\pi^-\pi^+\pi^-$ at rest, Nucl. Phys. **A690**, 567 (2001).
[69] D. V. Bugg, B. S. Zou, and A. V. Sarantsev, New results on $\pi\pi$ phase shifts between 600-MeV and 1900-MeV, Nucl. Phys. **B471**, 59 (1996).
[70] M. Bargiotti *et al.* (OBELIX Collaboration), Coupled channel analysis of $\pi^+\pi^-\pi^0$, $K^+K^-\pi^0$ and $K^\pm K^0_S\pi^\mp$ from $\bar{p}p$ annihilation at rest in hydrogen targets at three densities, Eur. Phys. J. C **26**, 371 (2003).
[71] V. V. Anisovich, V. A. Nikonov, and A. V. Sarantsev, Determination of hadronic partial widths for scalar isoscalar resonances $f_0(980)$, $f_0(1300)$, $f_0(1500)$, $f_0(1750)$ and the broad state $f_0(1530^{+90}_{-250})$, Phys. At. Nucl. **65**, 1545 (2002).
[72] N. N. Achasov and G. N. Shestakov, On the $f_0(1370)$ and $f_0(1520)$ resonances found in $\bar{N}N$ annihilation at rest, Phys. Rev. D **53**, 3559 (1996).
[73] J. Chen, X.-Q. Li, and B.-S. Zou, Bose symmetry interference effects of 4π final states, Phys. Rev. D **62**, 034011 (2000).
[74] A. D. Martin and T. D. Spearman, *Elementary Particle Theory* (North-Holland Publishing Co., Amsterdam, 1970).
[75] V. Mathieu and V. Vento, η-η' mixing in the flavor basis and large N, Phys. Lett. B **688**, 314 (2010).